Physicochemical properties and structure of titania-containing metallurgical slags: a review

Zhi-ming Yan[1], Xue-wei Lv[2], Zu-shu Li[1]

[1] WMG, University of Warwick, Coventry CV4 7AL, UK

[2] School of Materials Science and Engineering, Chongqing University, Chongqing 400044, China

* Corresponding Author:

Xue-wei Lv: lvxuewei@163.com

Zu-shu Li: Z.Li.19@warwick.ac.uk

Abstract

The titanium industry can hardly bypass the titania-containing slags, and the slag physicochemical properties are essential in the metallurgical reactor design and process control. The TiO_2-FeO based slags and TiO_2-SiO_2-CaO based slags are the main metallurgical slag systems in the titanium resource utilization processes. To elaborate the role of TiO_2 in the physicochemical properties of titania-containing metallurgical slags, the physicochemical properties including titanium redox ratio, liquidus temperature, viscosity, electrical conductivity, density, surface tension, thermal conductivity, and sulfide capacity were critically reviewed. Moreover, the property prediction models were briefly introduced with regards to the limitations of the existing models. The properties prediction models are still required to evolve since not all properties of titania-containing slags can be well modelled. As the slag structure has an intimate relationship with slag properties, the structural details of the titania-containing slag were investigated by using a combination of spectroscopic technologies, but the knowledge of the slag structure was not fully ascertained. The potential research fields related to the physicochemical properties and structure of the titania-containing slags were also suggested.

Keywords: titania-containing slag; physicochemical property; prediction model; slag structure

1. Introduction

Titanium has been considered as a rare metal for a short period of time because it is dispersed in nature and difficult to extract. However, its reserves are relatively abundant, ranking the tenth in all elements in the earth's crust [1, 2]. As a structural metal, titanium is the fourth largest consumer product after iron, aluminium and magnesium. There are hundreds of titanium minerals and compounds in the earth, while considering the reserves and ore grades, only a few of them have the value for industrial production [3]. Rutile and ilmenite are the main mineral raw materials used in the current industry for the extraction of titanium. Rutile is a titanium-rich mineral containing about 95 wt.% TiO_2, which is mainly stored in coastal areas such as beaches. The ilmenite ($FeO \cdot TiO_2$ or $TiFeO_3$) contains 40-65 wt.% TiO_2, which are commonly found in rock deposits with significant reserves for large-scale mining. Since 2020, the reserves of rutile and ilmenite are estimated to be about 46 and 770 million metric tons in the world, respectively [4]. Therefore, there is no doubt that ilmenite is the most important titanium resource and continues to dominate the future titanium industry. Ilmenite supplies about 90% of the world's demand for titanium minerals, with its world production of about 7.6 million metric tons in 2020 [4].

For industrial production, many metallurgical processes have been designed based on the characteristics of mineral resources. The typical processes developed by Quebec Iron and Titanium Corporation of Canada (QIT), Richards Bay Minerals of South Africa (RBM), Tinfos Titan and Iron KS of Norway (TTI) and Pangzhihua Steel Company of China (PSC) have their own characteristics, which are well documented by Sun et al. [5]. Figure 1 is the basic industry flow chart of titanium raw material utilization. Although there are differences among the various processes, the electric furnace (EF) is used in all the processes for melting and separation. Ilmenite minerals are often upgraded to titania slag via electro-smelting processes in electric arc furnaces (Ti-EAF slag) to produce the two main products - titanium dioxide (by sulphate or chloride processes) [6] and metallic titanium (by Kroll process) [7]. At the same time, semi-steel is the by-product [8]. The titanium reserves in China account for one-third of the world reserves and mainly exist as titaniferous magnetite [9]. The titaniferous magnetite is separated into iron concentrates and titanium concentrates by mineral beneficiation processing. Iron concentrates are utilized in the blast furnace (BF) ironmaking

process, and titanium concentrates are smelted in an electric furnace or used as the raw material for the sulphate process. In this process, about half of the titanium remaining in iron concentrates cannot be extracted and form the Ti-bearing BF slag. In recent years, a new process named the direct reduction-electric furnace smelting separation process (DR-EAF) has been suggested to fully recover the Fe, Ti, V, and Cr in the titanium-containing minerals. DR-EAF is considered to be an efficient way to utilize ilmenite minerals, while there is currently no large-scale industrial application. Meijer et al. [10] reported that the HIsarna process, a new smelting reduction process, offers the potential to smelt titano-magnetite ore directly but still in the pilot test. Currently, the TiO_2-FeO based electric arc furnace (EAF) slags and titano-silicate based BF slags are the main titania-containing metallurgical slag systems in the titanium resource utilization processes. Table 1 shows the typical chemical composition of titania-containing slag from different processes [5, 11, 12]. The total titania content (ΣTiO_2) in these slags varies greatly, from about 20 wt.% to 90 wt.%. The titania content in these titania-containing slags is typically expressed as ΣTiO_2 because the analytical methods for measuring the total titanium are fast and less cumbersome than the wet chemistry titration method required to measure Ti^{3+} [13].

Titanium metallurgical processes cannot bypass the titania-containing slags, and the properties of the titania-containing slags are essential in reactors design and metallurgical process control for efficient titanium extraction. This article aims to critically review the properties of titania-containing metallurgical slags in terms of the role of TiO_2. The potential research topics will be suggested for the physicochemical properties and structure of titania-containing slags.

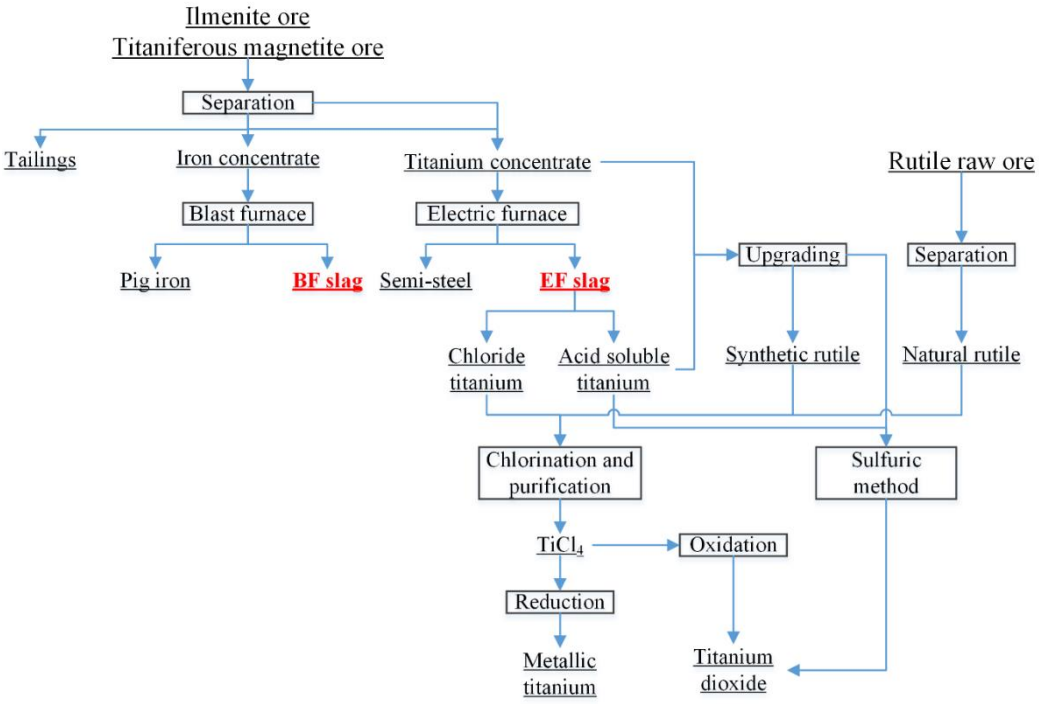

Fig. 1 Basic industry flow chart of titanium raw material utilization

Table 1 Typical chemical composition of titania-containing metallurgical slags from different processes (wt.%) [5, 11, 12]

Process		ΣTiO_2	FeO	CaO	SiO_2	Al_2O_3	MgO	MnO	Cr_2O_3	V_2O_5
QIT	EAF slag	80.00	9.00	0.60	2.40	2.90	5.00	0.25	0.17	0.56
RBM	EAF slag	85.50	7.50	0.14	1.50	2.00	0.90	1.40	0.22	0.40
TTI	EAF slag	77.40	7.60	0.66	5.35	1.19	7.92	-	0.07	0.25
DR-EAF	EAF slag	50.60	2.28	6.46	12.60	14.50	10.97	-	0.39	0.53
PSC	EAF slag	82.30	9.55	0.58	2.85	2.07	1.33	1.37	0.13	0.29
	BF slag	23.83	1.59	26.54	24.37	13.76	8.48	0.53	-	0.34

2. Physicochemical properties of titania-containing metallurgical slags

2.1 Titanium redox ratio

In titanium metallurgical processes, carbothermal reduction is the main method to separate the Fe and Ti from ilmenite/titaniferous-magnetite. The redox state of titanium must be discussed briefly as the presence of Ti^{3+} would obviously affect both physicochemical properties and thermodynamic behaviour of the titania-containing slags. The redox reaction can be written as [14]:

$$TiO_2 \leftrightarrow TiO_{1.5} + \frac{1}{4}O_2$$

$$\Delta G^{o} = 189{,}954 - 48.5T \quad (\mathrm{J/mol}) \qquad (1)$$

$$TiO_4^{4-} \leftrightarrow Ti^{3+} + \frac{7}{2}O^{2-} + \frac{1}{4}O_2 \quad (2)$$

where ΔG° is the standard Gibbs free energy, J/mol; and T is temperature, K.

Many investigators studied this equilibrium and showed a linear relationship between $-\log(X_{Ti^{3+}}/X_{Ti^{4+}})$ and $-\log(P_{O_2})$ with a slope of about -4 at constant temperature and composition [14-21], where $X_{Ti^{3+}}/X_{Ti^{4+}}$ is the molar ratio of Ti^{3+}/Ti^{4+} and P_{O_2} is oxygen partial pressure. The strong dependence of the equilibrium constant of reaction (1) on composition and temperature is clearly shown in Fig. 2. According to the work by Johnston [15], the $X_{Ti^{3+}}/X_{Ti^{4+}}$ ratio and oxygen partial pressure in Na_2O-$2SiO_2$ glasses with 1.5 wt.% TiO_2 were measured, and the results indicated that the Ti^{3+}/Ti^{4+} molar ratio is proportional to $P_{O_2}^{-1/4}$. Schreiber et al. [16] investigated the Ti^{4+}-Ti^{3+} equilibria in CaO-SiO_2-MgO-Al_2O_3-TiO_x systems, confirmed the relationship between the $X_{Ti^{3+}}/X_{Ti^{4+}}$ ratio and oxygen partial pressure, and reported that the $X_{Ti^{3+}}/X_{Ti^{4+}}$ ratio is favoured by decreasing slag basicity (w_{CaO}/w_{SiO_2}). Tanabe and Suito [17] measured the Ti^{4+}-Ti^{3+} distribution in CaO-TiO_x slags with more than 65 mol% TiO_x and found that the $X_{Ti^{3+}}/X_{Ti^{4+}}$ ratio decreases with increasing CaO concentration. The redox behaviour of titanium in CaO-SiO_2-TiO_x slag was studied by Tranell et al. [14] and Ariyo et al. [18]. Experimental results showed that the $X_{Ti^{3+}}/X_{Ti^{4+}}$ ratio with oxygen partial pressure followed the ideal behaviour, and the $X_{Ti^{3+}}/X_{Ti^{4+}}$ ratio increased with increasing temperature. The reduction reaction of TiO_2 to $TiO_{1.5}$ with the temperature dependence of the standard Gibbs free energy can be presented in Eq. (1). Since the reduction of TiO_2 is endothermic, the rise of temperature would favor Eq. (1) move to the right and stabilize titanium in the Ti^{3+} state. Tranell et al. [14] also reported that the $X_{Ti^{3+}}/X_{Ti^{4+}}$ ratio decreased with increasing basicity. From Eq. (2), the reduction of Ti^{4+} to Ti^{3+} would release free oxygen O^{2-} to depolymerize the melt. The increase in basicity would increase the O^{2-} in the melt, inhibiting the reduction reaction. According to the results from Tranell et al. [14], the difference in the logarithm values of the $X_{Ti^{3+}}/X_{Ti^{4+}}$ ratio is about 0.25 when temperature increases from 1570 to 1630 °C, while the value is about 0.65 when basicity decreases from 0.70 to 1.25. Ito and Sano [22] found that the $X_{Ti^{3+}}/X_{Ti^{4+}}$ ratio increased with increasing basicity for basicity less than one and decreased for basicity above one, which is in disagreement with the studies by Tranell et al. [14] and Morizane et al. [23]. The FeO-TiO_2-Ti_2O_3 slag is the main system of the ilmenite smelting process. Pesl and Eriç [20] and Geldenhuis and Pistorius [21] found that the relationship between the $X_{Ti^{3+}}/X_{Ti^{4+}}$ ratio and oxygen partial pressure is close to ideal for the slag systems investigated, and Ti_2O_3

concentration decreases with increasing FeO content. In a certain smelting process, the oxygen partial pressure is mainly governed by the Fe-FeO equilibrium in the slag [24], while the quality of the raw materials determines the basicity.

Kotzé [25] introduced the electronic polarizability to calculate oxygen activity for predicting the $X_{Ti^{3+}}/X_{Ti^{4+}}$ ratio in CaO-SiO_2-TiO_x slags and the results of this correlation agree well with the experimental data from Tranell et al. [14]. Hu et al. [19] provided a semi-empirical mathematical equation (Eq. (3)) based on their experimental data to present the relationship among oxygen partial pressure, slag composition and temperature for the FeO-TiO_2-Ti_2O_3 system.

$$\lg P_{O_2} = -15.66 - 2.07\lg\frac{w_{Ti_2O_3}}{w_{TiO_2}} + 0.54\lg w_{FeO} + \frac{7037.01}{T} \quad (3)$$

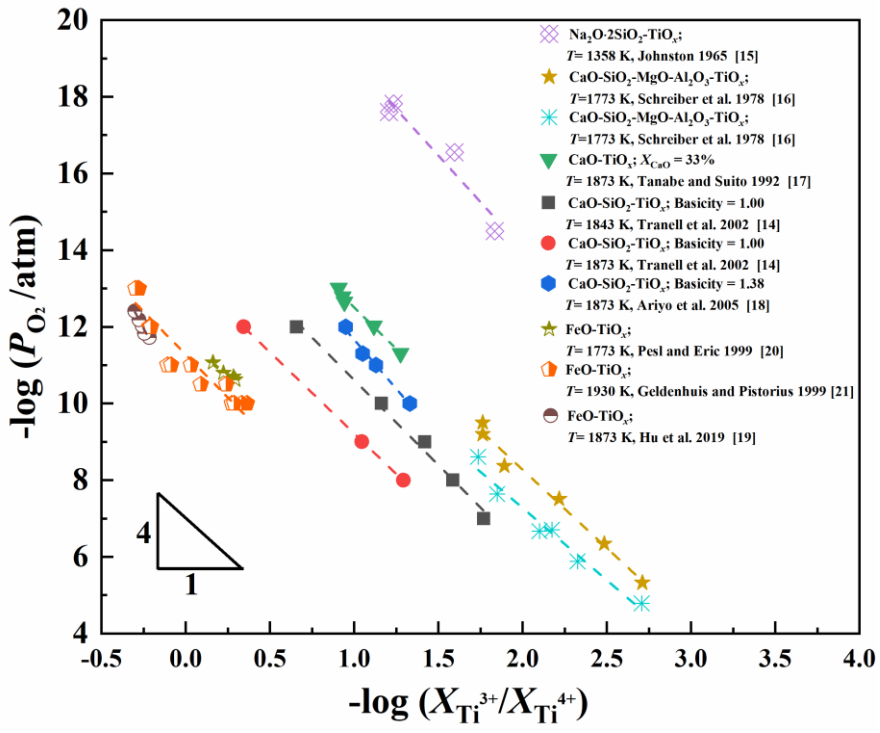

Fig. 2 Variation of redox ratio $(X_{Ti^{3+}})/(X_{Ti^{4+}})$ with oxygen partial pressure as a function of temperature (1 atm = 10^5 Pa)

2.2 Liquidus temperature

The liquidus temperature of the slag is an important property to the metallurgy processes since it is essential to maintain a flowing or running slag in most processes, and disasters can occur if the slag freezes in the vessel. The ilmenite smelting proceeds at high temperature due to the high melting point of the high titania slag. The exact liquidus relationship in this slag system is unclear, but a liquidus diagram calculated by FactSage is shown in Fig. 3. The square symbols reflect the typical composition of industrial high titania slags with a high

melting point near 1600 °C, and most of the solidified industrial slags located in the 'psb' phase area. Many researchers have noted that the M_3O_5 phase constitutes the largest part of the structure of the solidified industrial titania slag, with only small proportions of other phases (mainly rutile and silicates) [24, 26]. This M_3O_5 phase accommodates divalent and trivalent ions together with the tetravalent titanium, in a solid solution between compounds of the two basic forms $M^{2+}(Ti^{4+})_2O_5$ and $(M^{3+})_2Ti^{4+}O_5$ (the divalent ions: Fe^{2+}, Mg^{2+}, and Mn^{2+}, and the trivalent ions: Ti^{3+}, Cr^{3+}, Al^{3+}, and V^{3+}). Pesl and Eriç [20] studied the phase equilibria and thermodynamics of the FeO-TiO_2-Ti_2O_3 ternary system at 1500 and 1600 °C. The experiments were conducted by controlling the oxygen partial pressure with CO-H_2 mixture gas, and the samples in platinum or molybdenum crucibles were calibrated for more than 6 h before rapidly quenching them to capture the high-temperature phases. Their predicted liquidus isotherms for 1600 °C are plotted in Fig. 3 as broken lines. Seim [27] determined the liquidus temperature of $FeTiO_3$-Ti_2O_3-TiO_2 slag system from cooling curves captured by a spectropyrometer looking down onto the upper surface of the slag in an Ar atmosphere, using titanium metal and haematite additions to control the level of reduction. Seim [27] developed a model for calculating the liquidus isotherms of the system based on the measured liquidus temperature of the iron-saturated slags and expanding the thermodynamic dataset. The model is considered to predict the liquidus temperatures of the iron-saturated slags accurately. However, the measured liquidus temperature of the iron-unsaturated slags was unexpectedly and unexplainably lower and not used in the modelling process. The predicted liquidus isotherms by Seim for 1600 °C are also plotted in Fig. 3 as broken lines. Due to different experimental methods and conditions, the experimental results reported by Pesl and Eriç [20] and Seim [27] are quite different, resulting in inconsistent results predicted by models based on experimental data. The isotherm liquidus predicted by Pesl model and Seim model at 1600 °C together with all three isotherm sets shows a liquid slag field with three boundaries: a left phase boundary with the liquid slag + TiO_x phase field, a right phase boundary with the liquid slag + liquid iron phase field, and a boundary with liquid slag + 'psb' + liquid iron phase field. This diagram illustrates that the liquidus temperature decreases with increasing FeO content, indicating that the higher reduction yields a higher slag liquidus. The Ti^{3+}/Ti^{4+} ratio increases with increasing reduction degree at fixed FeO content, resulting in decreased liquidus until the Ti^{3+}/Ti^{4+} ratio crosses the low liquidus trough between TiO_2 and Ti_2O_3. In practice, FeO in the slag decreases and Ti_2O_3 simultaneously increases as the reduction progresses, and the net effect results in the increase in liquidus temperature [25].

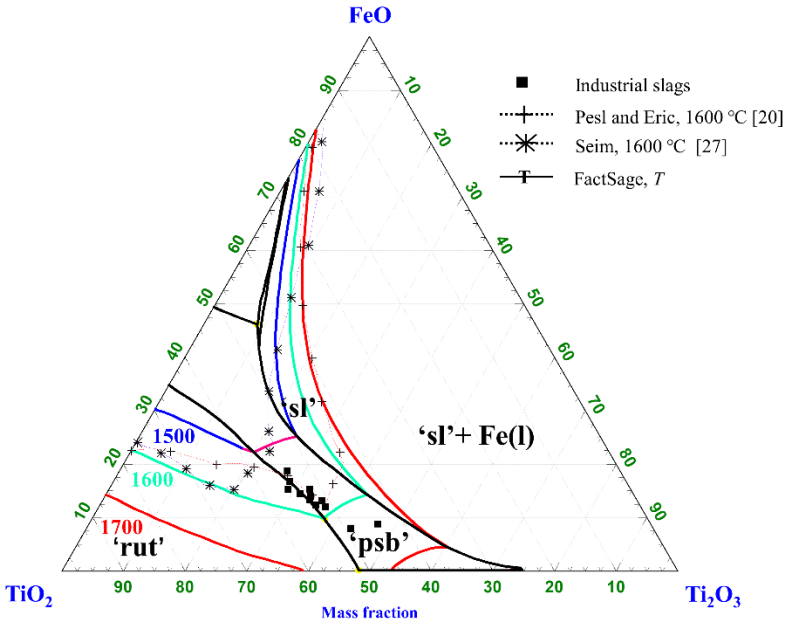

Fig. 3 Liquidus diagram of ilmenite smelting slags containing only FeO, TiO_2 and Ti_2O_3. 'sl'—Molten oxide (slag); 'psb'—pseudobrookite-M_3O_5 phase; 'rut'—rutile-based solid solution (TiO_2 with a small amount of Ti_2O_3 in solution); 'Fe'—metallic iron

In the study of titania-containing BF slags, metallurgists are more concerned about the free-running temperature (also named: fusibility temperature or crystallization temperature) rather than the liquidus temperature. Free-running temperature refers to the temperature corresponding to what condition the slag can flow freely, that is, the slag viscosity meets a certain condition. By definition, the free flow temperature is not the liquidus temperature, but the temperature is close and comparable to the liquidus, especially for the slags with strong crystallinity, such as titania-containing slags. Lv et al. [28] found that the free-running temperature shows a 'W' trend with increasing TiO_2 content from 0 to 50 wt.% in the SiO_2-CaO-TiO_2-8 wt.% MgO-14 wt.% Al_2O_3 BF type slag at fixed basicity and reported that the free-running temperature has peak values at the TiO_2 content of about 30 wt.%. From the liquidus diagram calculated by FactSage, as shown in Fig. 4, basicity at 1.1 is tangent to the 1450 °C liquidus when TiO_2 content is about 25 wt.%, which can explain why there is a peak at about 30 wt.% of the experimental results conducted by Lv et al. [28]. Wang and Yu [29] reported that the free-running temperature increases with increasing basicity in the normal operating range. These reported free-running temperature of high titania BF slag (TiO_2: 23−29 wt.%) ranges from 1380 to 1450 °C, which is about 80 °C higher than that of ordinary BF slags. The precipitation temperature of perovskite (the first precipitated phase: $CaTiO_3$) increases with increasing TiO_2 content and basicity, leading to the increase in the slag

liquidus. Recently, Pang et al. [30, 31] proposed an innovative slag system by substituting CaO with MgO to decrease the activity of CaO for lowering the precipitation temperature of perovskite. The free-running temperature first decreases with increasing the MgO/CaO ratio, indicating that the slag with high TiO_2 (30 wt.%) content could obtain a low liquidus temperature by using more MgO and less CaO content. However, since the BF slag contains a certain content of alumina, excessive MgO will increase the precipitation temperature of spinel ($MgAl_2O_4$), resulting in the increase in the slag liquidus. Therefore, the liquidus and the free-running temperatures of slag cannot be maintained in a suitable range by greatly increasing the MgO content. The reduction degree of TiO_2 plays an essential role in the BF process, and the free-running temperature increases rapidly because of a considerable amount of TiC and TiN generated by further reduction.

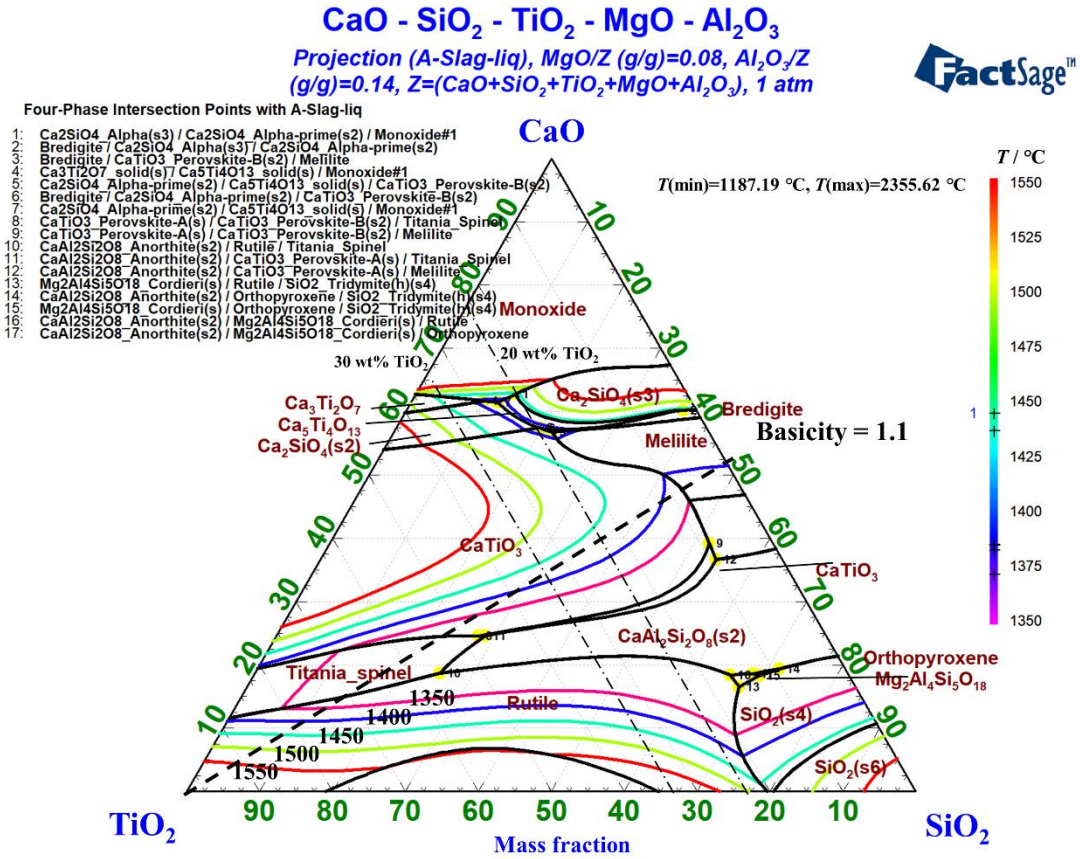

Fig. 4 Liquidus diagram of titania-containing BF slags (calculated by FactSage 7.3). Pseudo ternary diagram needs normalization when considering contents of MgO and Al_2O_3

2.3 Viscosity

The viscous behavior of slags has played an essential role in the titanium raw material utilization processes. In the electrical furnace smelting practice, a foamy TiO_2 slag can

suddenly occur, which is caused by a lack of fluidity associated with a change in slag temperature or composition during the smelting operation. A similar lack of fluidity has been noted in some blast furnace slags where high TiO_2 iron ores were smelted. The TiO_2 level was responsible for stickiness and hanging in the shaft. With all signs pointing to a viscosity problem, many works have been undertaken to study the viscosity of titania slags.

Frohberg and Weber [32] studied the viscosity of titania slags and reported that the addition of TiO_2 increased the fluidity of CaO-Al_2O_3-TiO_2, Al_2O_3-SiO_2-TiO_2, CaO-SiO_2-TiO_2 and CaO-Al_2O_3-SiO_2-TiO_2 slag systems, where the viscosity ranged from 5 to 40 dPa s. However, due to the utilization of graphite components in the measurement process, the measuring atmosphere was effectively reduced, so that the results were significantly higher than those of other researchers work [33-39]. As mentioned before, both the BF process and EAF process may involve titania-containing slag during the titanium metallurgical industry. In the BF slag, the main oxides are CaO, SiO_2, MgO, Al_2O_3, and TiO_2, accounting for more than 90%, while in the EAF slag, there are a certain amount of FeO and titanium suboxides because of the carbothermal reduction. Figure 5 shows the effect of TiO_2 on the viscosity of various slag systems under an inert atmosphere. As can be seen from Fig. 5, most of the studies focused on the BF type slag systems with TiO_2 content less than 50 wt.%, and the viscosity decreases as the TiO_2 content and the basicity increase. Ohno and Ross [33] found that both CaO and TiO_2 can decrease the viscosity of CaO-Al_2O_3-SiO_2-TiO_2 system, and the observation that TiO_2 can effectively reduce the viscosity of CaO-MgO-Al_2O_3-SiO_2-TiO_2 slag system is consistent with the work by Park et al. [34], Liao et al. [35], Sohn et al. [36], and Lv et al. [28]. Handfield and Charette [37] found that the addition of TiO_2 to slag decreased both the viscosity and the viscous activation energy. Kato and Minowa [38] used a slightly more acid slag and found that the addition of TiO_2 lowered the viscosity, but the viscous activation energy (E) was raised slightly. From the viewpoint of structure (Sect. 3), increasing TiO_2 content decreases the viscosity of titania-silicate-based slags because: (i) the Ti-O bond strength in TiO_4 tetrahdra or $TiOO_4$ units ($TiOO_4$ unit: one short Ti=O titanyl bond and four long Ti-O bonds) is weaker than that in SiO_4^{4-} tetrahedra; and (ii) some Ti^{4+} network formers transform into 6-fold coordinated network modifiers to decrease the degree of polymerization of the network. Regarding the viscosity of high titania EAF type slags, Handfield and Charette [37] studied SOREL slag (produced by QIT process; FeO 3.3−15 wt.% and TiO_2 67−80 wt.%). The viscosity of such slag was only 0.30 dPa s when it was fully molten, even lower than the viscosity of molten CaO, MnO, MgO and FeO near their melting

point. The 30 wt.% CaO-70 wt.% TiO_2 slag yielded an even lower value of 0.20 dPa s. Nikitin et al. [39] reported that the viscosity of FeO_x-TiO_2 system was less than 0.50 dPa s, and the increase in TiO_2 content caused a slight increase in viscosity. The structure of FeO-TiO_2 slags is not well understood yet, but according to the acidity of the oxides, the initial addition of TiO_2 would increase the viscosity. Hu et al. [11] studied the viscosity of PSC-EAF slag and found that the viscosities were less than 1.0 dPa s, and the addition of TiO_2 has no significant effect on the viscosity. Hu et al. [11] also noted that the critical temperature (where viscosity increases sharply) is only slightly below the slags' liquidus temperature. Though the composition of these high titania slags is different, their viscosities are very low and not sensitive to composition or temperature in a fully molten state.

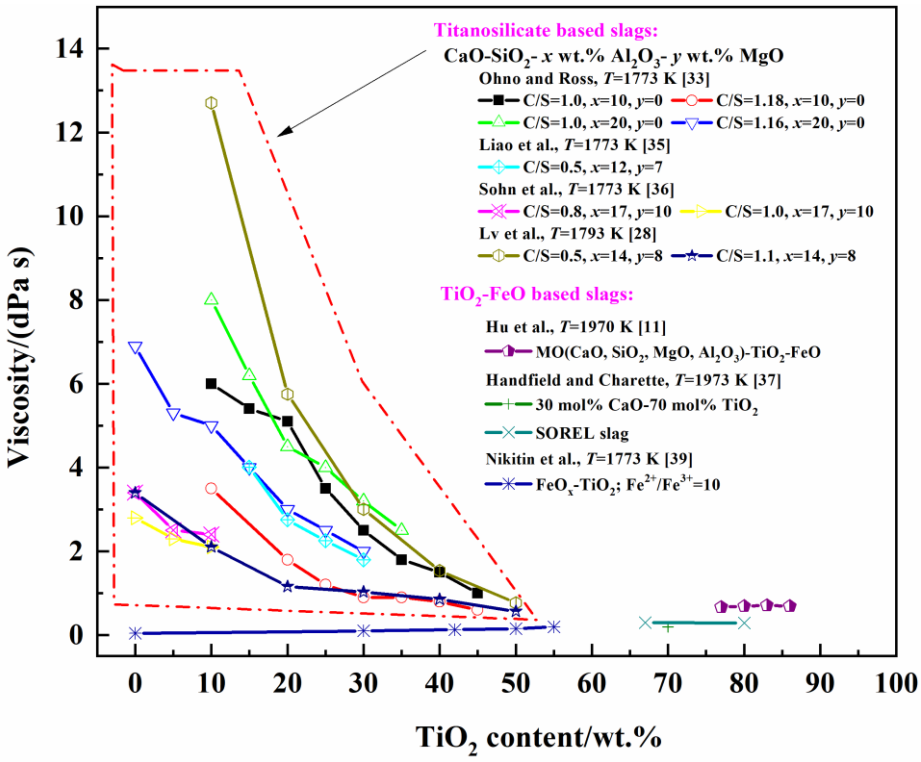

Fig. 5 Effect of TiO_2 on viscosity of titania slags. C/S = w_{CaO}/w_{SiO_2}

In the reduction conditions of the metallurgical processes, the TiO_2 may be partially reduced by carbon to form a series of reduction products such as Ti_2O_3, TiO, even TiC resulting in a more complicated viscosity behavior of the titania slag. Handfield et al. [40] investigated the effects of adding the sub-oxides Ti_2O_3 and TiO on a titanosilicate based slag. Their results showed that Ti_2O_3 and TiO decreased viscosity, while Ti_2O_3 was more effective than TiO. The slag fusibility temperature (the temperature when viscosity is 5 dPa s, defined by Handfield et al. [40]) decreased when the addition of either Ti_2O_3 or TiO was up to 10 wt.%, while further addition led to a rapid increase. The effect of Ti_2O_3 on viscous activation

energy was found to be greater than that of TiO_2, indicating that Ti_2O_3 is more basic and acts as a stronger network breaker. Xie et al. [41] studied the viscous behavior of titania-bearing BF slag under a reducing atmosphere and found that decreasing basicity resulted in accelerated reduction and thickening. The formation of Ti_2O_3 at the initial stage of reduction resulted in a slight decrease in viscosity, followed by a further reduction to TiO and formation of TiC, and viscosity increased rapidly. The fusibility temperature of the basic slag ($w_{CaO}/w_{SiO_2} > 1.0$) was decreased, while that of the acid slag ($w_{CaO}/w_{SiO_2} < 1.0$) was increased during the reduction. Ohno and Ross [33] observed that the thickening rate was faster in more acid slags, while their reduction rate was slower, indicating that the relationship between thickening rate and reduction rate is not simple. In the work with more complex slags by Van der Colf and Howat [42], a minimum viscosity was reported after about 30 min reduction, and after that, the more basic slags thickened more rapidly. They also pointed out that the slag liquidus temperature during reduction was not only determined by basicity but also partly by the nature of the primary precipitated phase of the initial slag. Bai [12] conducted a systematic study on the physicochemical properties of titania BF slag. It was found that the viscosity would not increase in the oxidation atmosphere or neutral atmosphere. However, under reduction conditions, sub-oxides (Ti_2O_3 and TiO) productions cause a decrease in viscosity due to the structural changes and a lower fusibility temperature. Wang and Yu [29] reported that the increase in temperature accelerates the reduction and increases the formation rate of TiC/TiN, resulting in an increase in viscosity. In the current BF process for smelting titaniferous magnetite ore, some plants use a blend of titano-magnetite ore with the normal iron ore to limit the TiO_2 content in the slag (less than 23 wt.%) to inhibit the excessive reduction [30, 31]. In the EAF slag, although the presence of FeO hinders the formation of TiC, the increase in reduction degree increases the liquidus temperature of high titania slag, and the solid phase may precipitate.

Various models for slag viscosity prediction have been developed in the past decades. The details and limitations of these models have been well documented [43-47]. However, few models could accurately estimate the viscosity of titania-containing slags. A brief summary of the viscosity models involving TiO_2 is presented in Table 2. It should be noted that the average relative errors (Δ) in Table 2 are from their test results in a specific composition range. Riboud et al. [48], based on Weymann-Frenkel relation, expressed the activation energy as the linear addition of network former components (SiO_2+P_2O_5+ZrO_2+TiO_2). The model established by Iida et al. [49] divides all the oxides into acidic oxides, basic oxides and

amphoteric oxides, using the basicity index to consider the network structure of the slag. TiO_2 is classified into acidic oxides in both of the above models. The estimated viscosity increased with the addition of TiO_2, which disagreed with the experimental data. Urbain model [50, 51] is also based on Weymann-Frenkel relation, expressing the activation energy with composition by a polynomial expression; the TiO_2 is treated as a network modifier. Yan et al. [28] reported that the calculated viscosity by the Urbain model exhibits a significant deviation compared with the measured viscosity data at high TiO_2 content in BF slags. Mills and Sridhar [52] developed a viscosity model based on corrected optical basicity, while this model was found not to perform very well. The model proposed by Zhang et al. [53] described by Arrhenius law and the oxygen ion related to Ti^{4+} is assumed to a new type of oxygen. However, the calculation of oxygen fraction relies on assumption and lacks theory support [44, 54]. Yan et al. [55] developed a structure-based viscosity model which is capable of predicting the viscosities in the CaO-MgO-Al_2O_3-SiO_2-TiO_2 systems with wide composition and temperature ranges. In recent years, with the development of computer technology, the calculation of the physicochemical properties of the slags based on computer simulation methods (i.e., density functional theory, first principles or molecular dynamics) has attracted the attention of researchers. Some researchers have made effective attempts to calculate the viscosity of slags via the molecular dynamics simulation method [56-58]. It should be noted that all of these models mainly deal with fully melted slags. Hu et al. [59] developed a viscosity model based on the modification of the Vogel-Fulcher-Tammann (VFT) equation for high titania EAF slag system, which is suitable for the slag containing Ti_2O_3 even below the critical temperature. In industrial smelting, the slag bath is likely to contain some solid phases (i.e. unreacted reagent, precipitates, and TiC/TiN). The existence of the solid phases leads to significant deviations in the viscosity model developed based on the fully molten state. The deviation depends on the solid phase volume fraction and the solid phase particle shape and size. The Einstein-Roscoe equation provides an opportunity to introduce the changes in flow behavior due to the solid particles. It has been widely used to predict solid-liquid phases slag viscosity due to its simple form [60-63].

Table 2 Summary of viscosity models involving titania-containing slags

Source	η-T relationship	Model description	Slag system and Δ
Urbain et al. 1981, 1987 [50, 51]	Weymann-Frenkel	Glass formers (G): SiO_2, P_2O_5, etc. Network modifiers (N): CaO, MgO, TiO_2, etc.	Various slags, Δ=25%

		Amphoterics (A): Al_2O_3, Fe_2O_3, etc. $\eta = AT\exp(B/T)$ $\ln A = -(0.293B + 11.571)$ $B = B_0 + B_1 X_G^* + B_2 (X_G^*)^2 + B_3 (X_G^*)^3$ $B_i = a_i + b_i\alpha + c_i\alpha^2$ (i=0, 1, 2, 3) $\alpha = x_G/(x_N + x_A)$ Where A and B are composition-dependent constants, X_G^* is the mole fraction of glass former, a_i, b_i, and c_i are fitting constants.	
Riboud et al. 1981 [48]	Weymann-Frenkel	'SiO$_2$' group: SiO_2, P_2O_5, TiO_2, etc. 'CaO' group: CaO, MgO, FeO, etc. 'Al_2O_3' group: Al_2O_3, etc. 'CaF_2' group: CaF_2 'Na_2O' group: Na_2O, K_2O, etc. $\ln A = -35.76X_{Al_2O_3} + 1.73X_{CaO} + 7.02X_{Na_2O} + 5.82X_{CaF_2} - 19.81$ $B = 68.88X_{Al_2O_3} - 23.896X_{CaO} - 39.159X_{Na_2O} - 46.356 + 31X_{CaF_2}$ where X_i is mole fraction of component i.	Mould flux, Δ=30%
Mills and Sridhar 1999 [52]	Arrhenius	Corrected optical basicity (Λ_{corr}) is a measure of depolymerization $\ln A = -232.7\Lambda_{corr}^2 + 357.3\Lambda_{corr} - 144.2$ $\ln(B/100) = -1.77 + 2.88/\Lambda_{corr}$	Various slags, Δ=34%
Iida et al. 2000 [49]	Arrhenius	$\eta = A\eta_0\exp(E/B_i^*)$ $\eta_0 = \sum \eta_{0i} X_i$ $B_i^* = (\sum(\alpha_i W_i)_B + \alpha_{Fe_2O_3}^* W_{Fe_2O_3})/(\sum(\alpha_i W_i)_A + \alpha_{Al_2O_3}^* W_{Al_2O_3} + \alpha_{TiO_2}^* W_{TiO_2})$ where B_i^* is modified basicity index; η_{0i} is hypothetical viscosity of pure component i; α_i is specific coefficient; and W_i is mass percentage of component i; The subscripts A and B represent acidic oxide and basic oxide, respectively; α_i^* is the modified specific coefficient indicating the interaction of the amphoteric oxide with other components.	Mould fluxes, Δ=25%
Zhang et al. 2014 [53]	Arrhenius	$\ln A = k(E - 572{,}516) - 17.47$ $k = \sum_{i,j\neq SiO_2}(X_i k_i)/\sum_{i,j\neq SiO_2}(X_i)$ $E = (572{,}516 \times 2)/(n_{O_{Si}} + \Sigma\beta_i n_{O'})$ where k_i is model parameters; $n_{O'}$ is number of different types of oxygen; and β_i describes deforming ability of bond around corresponding unit.	Various slags; CaO-SiO_2-MgO-Al_2O_3-TiO_2, Δ=16%
Yan et al. 2018 [55]	Frenkel's kinetic theory	$\eta = (2/3)N_h R_h (2\pi mkT)^{\frac{1}{2}}\exp(\frac{E}{RT})$ $E = a + \sum_{n=1}^{3}(b_{i,n}(NO_i^0)^n + c_{j,n}(NO_j^-)^n)$; $(i = Si^{4+}, Al^{3+}, Ti^{4+}; j = Ca^{2+}, Mg^{2+})$ NO^0 is fraction of bridging oxygen NO^- is fraction of non-bridging oxygen NO^{2-} is fraction of free oxygen	CaO-SiO_2-MgO-Al_2O_3-TiO_2 BF slag, Δ=20%
Hu et al. 2021 [59]	Vogel-Fulcher-Tammann	$\lg\eta(T,x) = \lg\eta_\infty(x) + A(T,x)/(T - T_0(T,x) = A + B/(T - C)$	TiO_2-FeO, TiO_2-FeO-Ti_2O_3, and TiO_2-FeO-MO_x (M =Ca, Si, Mg) high titania slag systems.

		$A = \lg\eta_\infty(x) = \sum_{i=1}^{n} r_i x_i$ $B = A(T,x) = \sum_{i=1}^{n}\sum_{j=1}^{m}(x_i x_j(a_{ij} + b_{ij}T)$ $C = T_0(T,x) = \sum_{i=1}^{n}\sum_{j=1}^{m}(x_i x_j(c_{ij} + d_{ij}T)$ where r_i, a_{ij}, b_{ij}, c_{ij}, and d_{ij} are model fitting parameters.	EAF slag, Δ=19%
Einstein, 1906 [60]; Roscoe, 1952 [61]; Zhen et al., 2015 [62]; Zhang et al., 2015 [63]	Einstein-Roscoe	$\eta = \eta_0(1 - af)^{-n}$ η_0 is viscosity of solid-free melt; f is volume fraction of solid particles; and a and n are constants.	Slags with solid phases

$\Delta=(\sum\delta)/N$, where $\delta=(\eta_{meas}-\eta_{calc})/\eta_{meas}\times100\%$; η_{meas} is measured viscosity; η_{calc} is calculated viscosity; and N is number of measurements

2.4 Electrical conductivity

Electrical conductivity directly affects the power supply and energy distribution in the electric furnace process of titanium slag production. The heat required for slag melting is mainly supplied by the resistance heat generated by the current passing through the slag and determined by the resistivity (the reciprocal of the conductivity) of slag. The electrical conductivity of slags is contributed by two mechanisms: ionic conduction and electronic conduction. Figure 6 shows the effect of TiO_2 on the electrical conductivity of various titania slag systems. Most of the titania slags have yielded such high electrical conductivity that electronic conduction is clearly predominating over ionic conduction. For example, in the industrial slag systems reported by Grau and Poggi [64], Desrosiers et al. [65], and Hu et al. [66], the electrical conductivity varied from 20 to 200 Ω^{-1} cm^{-1}. In the FeO-TiO_2 system investigated by Mori [67], the electrical conductivity showed a minimum of 30 Ω^{-1} cm^{-1} at 40 mol% TiO_2, which is in qualitative agreement with the results by Denisov et al. [68] and Nikitin et al. [39]. The electrical conductivity of pure FeO was obtained by Inouye et al. [69] with the value of almost 300 Ω^{-1} cm^{-1} and above 200 Ω^{-1} cm^{-1} for pure TiO_2 by Reznichenko [70]. The addition of other components does lower conductivities appreciably [71-73], but even in slag bearing as much as 40 wt.% of CaO, SiO_2, MgO, and Al_2O_3 from the work by Shi and Wang [73], the conductivities at 1713 K were more than 5 Ω^{-1} cm^{-1}, so that here electronic conduction appears to be predominant. Since Fe, Mn and Ti are transition metal elements, a similar mechanism is probably operative in most of these slags due to one or all of them. A theory for electronic conduction in transition metal oxides glasses was proposed

by Mott [74], which was referred to as “small polaron hopping” or “Mott’s transition”. Based on this mechanism, conduction can be performed by jumping electrons from low valence cations to adjacent high valence transition metal cations. Therefore, both low valence and high valence cations are required for this mechanism. The studies by Evseev and Filippov [75], Mori [76], and Churkin et al. [77] reported that the values of electrical conductivity in their work in an inert atmosphere (no low valence cations) were less than 1.0 Ω^{-1} cm^{-1}, clearly in the ionic conduction range, and Ca^{2+} cations being considered as the mobile ions. Conductivity increased with TiO_2 content at fixed basicity and increased with basicity at fixed TiO_2 content. The cations concentration and mobility and the resistance of movement of cations by the network structure in the slag are the main reasons that affect the ionic conduction.

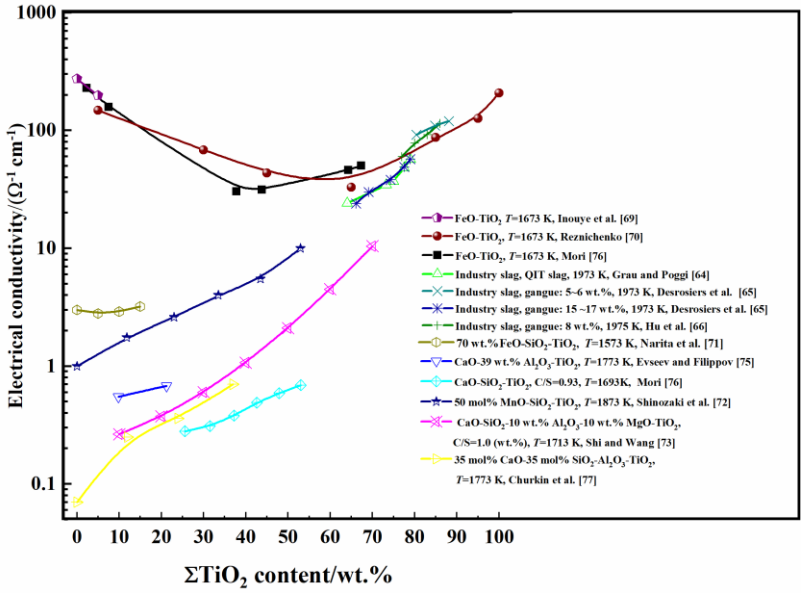

Fig. 6 Effect of TiO_2 on electrical conductivity of titania slags, C/S = w_{CaO}/w_{SiO_2}

As to the effect of reduction, it is foreseeable that a certain degree of reduction will lead to an increase in conductivity based on “Mott’s transition” theory. It can be confirmed by Lepinskikh et al. [78] that conductivity is increased by a slight reduction. There is an inverse relationship between the FeO and Ti_2O_3 contents when partially reduced in the slags bearing both iron and titanium oxides, which obviously affects the conductivity [79]. From this point of view, the FeO content can be considered as a control parameter in the industrial situation. Decreased temperature tends to intensify the network and restrain the ionic movement; thus, the decreased temperature would be expected to decrease the conductivity. However, in our previous work [66], an interesting phenomenon was reported, as shown in Fig. 7, that the conductivity decreases with decreasing temperature at the fully melting stage (Stage I) as

expected. When the temperature drops below the liquidus, the conductivity increases as the precipitation of the rutile phase (Stage II) due to the high conductivity of TiO_2 at high temperature. With the temperature further decreasing, the electrical conductivity of the slag decreases again because of the precipitation of other phases and the rapid decrease in the amount of liquid phase (Stage III).

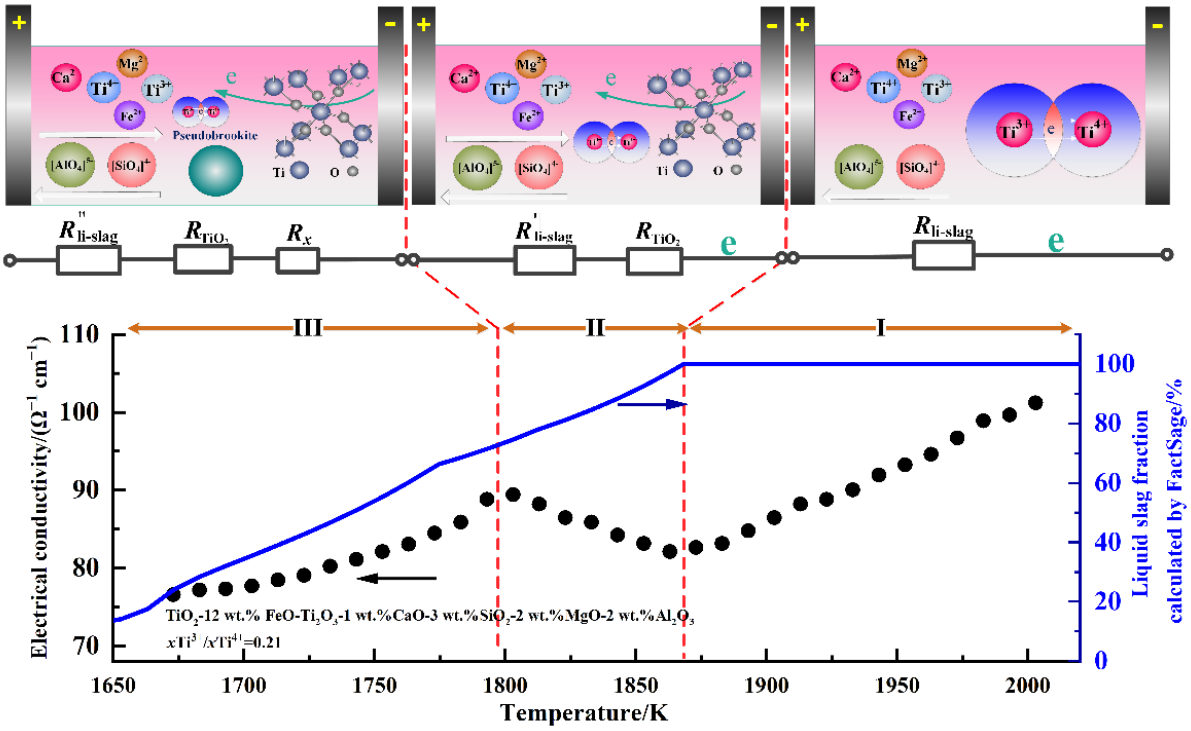

Fig. 7 Effects of temperature on electrical conductivity of titania slag (dot line), liquid slag fraction (blue line), and electronic conduction mechanism of electrical conductivity of titania slag in different stages (I, II, III). $R_{li\text{-}slag}$—Resistance of liquid slag; R_{TiO_2}—resistance of precipitated rutile (known as a semi-conductor); R_x—resistance of other precipitated phases, such as pseudobrookite. (Data from Ref. [66])

There are few models for calculating the electrical conductivity/resistivity of slags and glasses. Jiao and Themelis [80] obtained an empirical relation for CaO-MgO-MnO-SiO_2 slags at 1500 °C, but a limited application for the industrial slags. Zhang et al. [81, 82] recently reported two models for predicting the electrical conductivity of some silicate slags: one is based on the structure of slags by using optical basicity, and the other one builds the relationship between the viscosity and electrical conductivity. These models are suitable for silicate slag in the ionic conduction range; however, the titania slag needs to consider the electronic conduction. There is currently no available model for titania slag. Thus, the electrical conductivity model development for the titania slags is in its infancy.

2.5 Density and partial molar volume of TiO_2

The density of slags is important in slag/metal separation, determining the slag volume and kinetics in the metallurgical process. In molten slag systems, the density calculation needs to consider the mixing enthalpy. However, for high titania slag (FeO-TiO_x) with only a small deviation from the ideality, the weighted average of the density of pure oxides is sufficient [83]. The density of TiO_2 and Ti_2O_3 liquid near the melting point was measured by Dingwell [84] and Ikemiya et al. [85], and extrapolated to 1600 °C, the densities were taken as 3.31 and 4.0 g/cm^3, respectively. The density of FeO at 1600 °C was reported as 4.4 g/cm^3 based on the measurements done by Xin et al. [86]. Therefore, the typical high-TiO_2 slags have a density ranging from 3.5 to 3.7 g/cm^3, and the higher TiO_2 content results in the lower slag density [25]. For the CaO-SiO_2-MgO-Al_2O_3-TiO_2 BF type slag, Liu et al. [87] reported that the density increased firstly with increasing the TiO_2 content from 0 to 23 wt.%, and then decreased once the TiO_2 content exceeded 23 wt.% at 1400 °C at a fixed basicity by using the dispensed drop method, while Pang et al. [88] found that the density decreased with increasing TiO_2 from 20 to 30 wt.% without turning point via the Archimedean principle. The density was in the range of 2.60 to 2.90 g/cm^3.

Usually, the density of slag provided relies on some developed models. Experimental data are scarce due to the high reactivity of molten slag and the technical difficulty of taking precise measurements at elevated temperatures; on the other hand, the developed models can determine the density of many molten slags with reasonable accuracy. According to the definition, the density of slag can be calculated by Eq. (4):

$$\rho = \frac{\sum X_i M_i}{V_{\mathrm{m}}} \tag{4}$$

where ρ is the density of the slag; X_i is the mole fraction of component i; M_i is the molar mass of component i; and V_{m} is the molar volume of the slag. The main task of most density models is the calculation of the molar volume of slag, as shown in Table 3. Therefore, in order to calculate the density of slag bearing titania, the partial molar volume of TiO_2 is required. Nelson and Carmichael [89] measured the volumes of more than twenty titanosilicate melts with two to eight components and reported a constant value of 24.9 cm^3/mol at 1500 °C for the partial molar volume of TiO_2. In fact, the value of 24.3 cm^3/mol fits very well with the volume of pure TiO_2 measured at higher temperatures by Dingwell [84]. The molar volume for hypothetical glass with 4-fold coordinated Ti is about 25 cm^3/mol. Lange and Carmichael [90] also reported that the value is lower than their own measurements on Na-titanosilicates,

which reported a molar volume of 28.3 cm^3/mol at 1500 °C. Such different values reflect the large structural differences between the manners in which Ti interacts with the various cations. The cations (alkali metals cations and alkaline earth cations) and TiO_2 content led to the diversity of Ti-O polyhedral, which makes the partial molar volumes of TiO_2 markedly depend on the composition. In models of Lange and Carmichael [90], Mills and Keene [91], and Linard et al. [92] (Table 3), the recommended value of the partial molar volume of TiO_2 at 1500 °C is near 24.0 cm^3/mol in titanosilicate-based slags. Based on the three models, the densities of CaO-SiO_2-8 wt.% MgO-14 wt.% Al_2O_3-TiO_2 (basicity = 1.10) at 1500 °C with different TiO_2 contents were calculated and compared with the experimental data reported by Liu et al. [87] and Pang et al. [88]. As shown in Fig. 8, the density increases with increasing TiO_2 content via the models' prediction; however, it shows an opposite result from the experiment when TiO_2 content is higher than 20 wt.%. The difference in the measured values is due to the difference in temperature and measurement method. According to the partial molar volume of oxides (also see Fig. 8), it is easy to find that the density of TiO_2 is higher than that of other oxides. The density of the slag will increase when the dense component TiO_2 is initially added to the slag. With increasing the TiO_2 content in the slag system, the structure of the slag becomes loose since the Ti-O bond is longer than the Si-O bond and the concentration of Ti^{4+} in higher oxygen coordination numbers increases, resulting in the decrease in slag density.

Table 3 Summary of models to calculate densities of titania-containing slags

Source	Description	Slag system	Reported Δ/%
Lange and Carmichael [90]	$V_m = \sum X_i V_i + X_{Na_2O} X_{TiO_2} V_{Na_2O-TiO_2}$ (V_{TiO_2}=23.98 cm^3/mol, dV/dT=7.24× 10^{-3} K^{-1} based on 25 liquidus + 2 CaO-TiO_2-SiO_2 liquidus) V_{TiO_2}=28.32 cm^3/mol, dV/dT=8.76× 10^{-3} K^{-1} based on 25 liquidus+2 Na_2O-TiO_2-SiO_2 liquidus)	Slags (CaO, SiO_2, MgO, Al_2O_3, MnO, FeO, Fe_2O_3, Na_2O, K_2O, **TiO_2**)	/
Mills and Keene [91]	$V_m = \sum X_i V_i$ where V_i values are given at 1773 K (V_{TiO_2}=24 cm^3/mol, dV/dT=10^{-2} K^{-1})	Slags (CaO, SiO_2, MgO, Al_2O_3, MnO, FeO, Fe_2O_3, Na_2O, K_2O, **TiO_2**)	2-3
Linard et al. [92]	$V_m = \sum X_i V_i + \sum_i v_{ij}^{xs} X_i X_j$ where (v_{ij}^{xs}) reflect excess volume contribution of interactions between each pair of components of the system (V_{TiO_2}=23.88 cm^3/mol, dV/dT=7.24 × 10^{-3} K^{-1})	Molten glasses (Most oxides including **TiO_2**)	4

Values in parentheses are partial molar volume of TiO_2 at 1500 °C and its temperature dependence

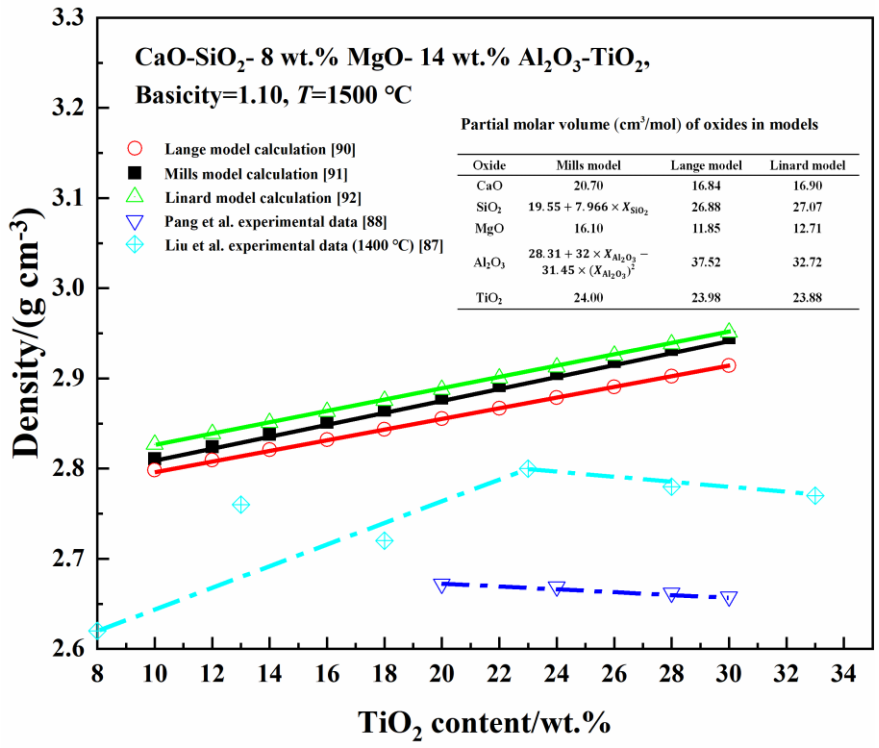

Fig. 8 Effect of TiO_2 on density of CaO-SiO_2-8 wt.% MgO-14 wt.% Al_2O_3-TiO_2 slags at 1500 °C

2.6 Surface tension and slag foaming

The surface tension of slag is important because it affects many metallurgical processes. The physical meaning of surface tension can be understood as the energy consumed to generate a unit area interface between liquid and gas. The surface of the oxides is mainly occupied by oxygen ions. Because the radius of the oxygen ions is larger than that of the cations, the surface tension of the slag is mainly determined by the interaction between the surface oxygen ions and neighbouring cations. Oxides with small cation ionic potentials (Z/r) and low ionic bond fraction have lower surface tension. Surfactants tend to be materials with low surface tension. The surface tensions of slags are dependent upon the concentrations of surfactants present. Mills [43] provided the suggested surface tension values of pure slag components at 1500 °C, as shown in Table 4. The principal surfactants in slags are B_2O_3, K_2O, Na_2O, SiO_2, and CaF_2. In titania slag systems, as shown in Fig. 9, the TiO_2 also acts as a surfactant to reduce the surface tension of slag. As the reduction reaction progresses during the ilmenite smelting process, the surface tension of slag will decrease due to the enrichment of TiO_2, and then the surface tension will increase with the increase in Ti_2O_3. Kozakevitch [93] investigated the FeO-TiO_2 system, Bochorishvili and Yakobashvili [94], Popel et al. [95], and Evseev and Filippov [75] studied the CaO-TiO_2-Al_2O_3 systems, and Liu et al. [96], Pang et al. [88] and Zhu et al. [97] investigated the surface tension of CaO-SiO_2-TiO_2-Al_2O_3-MgO

BF-type slags. All results suggested that increasing TiO_2 content results in a decrease in the surface tension. It should be noted that there is almost no surface tension data of high titania slag when the TiO_2 content in slag is higher than 50 wt.%.

Table 4 Surface tension δ of pure slag components at 1773 K

Oxide	SiO_2	CaO	BaO	MgO	FeO	MnO	Al_2O_3	Na_2O	K_2O	**Ti_2O_3**	**TiO_2**	Fe_2O_3	CaF_2	B_2O_3
δ/(mN m^{-1})	260	625	560	635	645	645	655	295	160	**610**	**360**	300	290	110

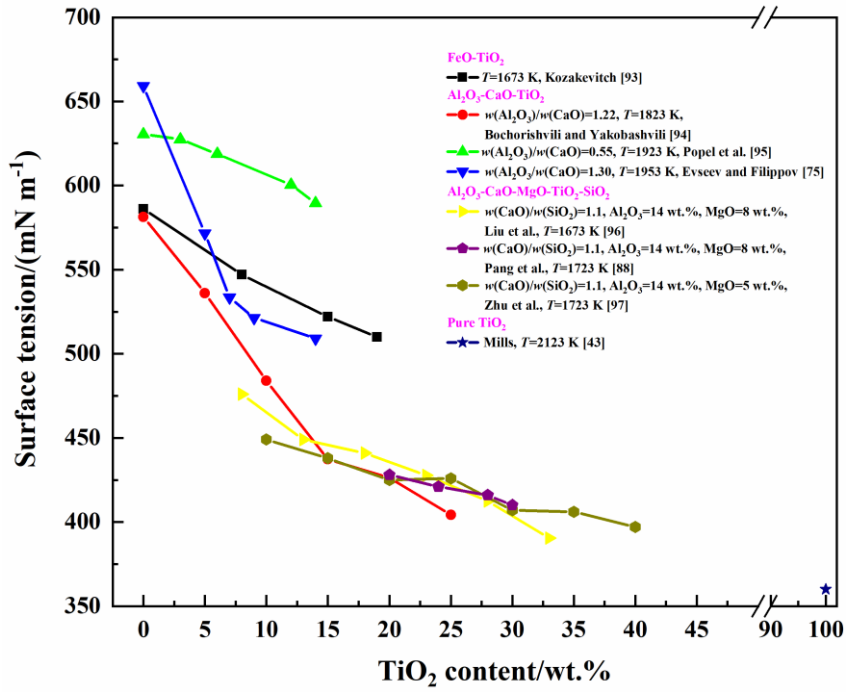

Fig. 9 Effect of TiO_2 on surface tension of titania slags

Boni and Derge [98] conducted an initial attempt to predict the surface tension of multi-component slag using the additivity rule. Mills [99] modified the additivity rule model by considering the partial molar contribution of the surfactant. Nakamoto et al. [100] developed a model based on the neural network computation, which is best applied to ternary silicate melts but would be less useful when applied to all slags. Tanaka et al. [101-103] reported a model based on the Butler equation and ionic radii for cations. This model takes radii of cations and anions into account and the partition of ions between bulk and surface, which is found to work successfully for a large number of slag systems. Liu et al. [96, 104] extended the Butler equation model to FeO-TiO_2-Ti_2O_3-*X* (*X*=CaO, SiO_2, MgO) slag systems and CaO-SiO_2-TiO_2-Al_2O_3-MgO BF-type slag and achieved good prediction results.

A foam slag is a heterogeneous medium consisting of gas bubbles dispersed in a slag. In the modern EAF steelmaking process, slag foaming has become an important feature with lots of benefits, including stabilizing the arc, shielding the refractory from the arc, acting as a thermal insulator, and improving productivity and energy efficiency. However, the ilmenite electro-smelting process usually adopts open arc operation due to the high electrical conductivity of high titania slag; thus, the massive slag foaming will cause a short circuit and force a furnace shutdown. For smelting titania ore in BF, the slag foaming affects the smooth operation and reduces the production efficiency. Understanding the foaming mechanism of titania-containing slag helps to control the smelting processes accurately. The formation of slag foaming and its relative stability are strongly influenced by the gas evolution rate, as well as the viscosity and surface tension. The higher surface tension of the slag means the higher energy required to create foams. The foam stability depends on the drainage rate of the liquid film between the bubbles; the lower viscosity means the faster drainage rate. Consequently, slags with lower surface tension and high viscosity are susceptible to foaming in processes involving extensive gas evolution. Suspended solid particles in the liquid will also increase the relative stability of the foam by increasing the apparent viscosity of the medium and by retarding the coalescence of the bubbles on which the solid particles are attached by the surface tension. Although the titania slags have low viscosity in a molten state, the presence of solid particles such as reducing agent (residual carbon), reduction product (TiC/TiN), and the precipitated phase (perovskite, rutile) will increase the apparent viscosity of the slag during the smelting process. Moreover, the surface tension of titania slags decreases with increasing TiO_2 content. Therefore, slag foaming is easy to occur in the ilmenite smelting process and BF process with feeding titania ore.

2.7 Thermal conductivity and heat capacity

In the ilmenite electro-smelting process, the titania slag with high activity is corrosive to refractory materials. Hence, the furnace wall is protected by a freeze lining of solid slag. Thermal conductivity directly affects the formation of the freeze lining in the furnace. Thus, the accurate thermal conductivity value of titania slag is essential for process simulation and operation. Kotzé and Pistorius [105] provided a linear function ($k_{\text{slag}} = 0.00175T + 0.3$ (W m^{-1} $℃^{-1}$)) for high titania slag blocks from 400 to 1500 °C, which gives a thermal conductivity range of 1.0 to 3.0 W m^{-1} $°C^{-1}$. In their work, heat capacity equations of solid and liquid titania slags were built for the specific slags studied. Heimo et al. [106] measured the thermal conductivity and heat capacity of three titania slags from room temperature to

1100 °C and reported that the thermal conductivity and heat capacity of the slags increase with temperature: thermal conductivity increased from 1.2 to 2.4 W m^{-1} $°C^{-1}$, and the heat capacity increased from 700 to 1100 J kg^{-1} $°C^{-1}$. No experimental results of thermal conductivity of molten titania slags were found in the literature.

2.8 Sulfide capacity and optical basicity

In the ilmenite electro-smelting process, the semi-steel is the by-product. In the BF ironmaking process and newly developed processes, those processes occur in the use of ilmenite/titano-magnetite in the production of iron and steel. Sulfur is a well-known harmful element in steel products, and slags play a significant role in the desulfurization of the metal in these processes. Since the sulfide capacity was proposed by Fincham and Richardson [107], many studies have been carried out on the sulfide capacity of metallurgical slags, but a little research has been performed on the sulfide capacity of titania slags, especially for the slag with high titania. Figure 10 shows the effect of TiO_2 on the sulfide capacity of titania slags. Tang and Xu [108] and Ling et al. [109] investigated the effect of TiO_2 on the sulfide capacity of BF-type slags and reported that the sulfide capacity decreases with increasing TiO_2 content. In the CaO-SiO_2-TiO_2(-MgO-Al_2O_3) systems conducted by Ghita and Bell [110] and Brown et al. [111], the sulfide capacity increases with increasing basic oxides content (i.e., FeO, CaO, and MgO) and decreases when substituting the TiO_2 by SiO_2 or Al_2O_3 at fixed basic oxides content. From the experimental results of MnO-TiO_2-SiO_2 system by Ito et al. [112], the increase in TiO_2 content decreases the sulfide capacity when MnO/SiO_2 molar ratio is about 2.0. Sommerville and Bell [79] concluded the desulfurization capabilities of TiO_2 weaker than those of MnO, CaO, MgO, and FeO, but stronger than those of Al_2O_3 and SiO_2. No reports were found in the open sources on the effect of titania sub-oxides (Ti_2O_3 and TiO) on the sulfide capacity of titania slags. However, it should be noted that Tang and Xu [108] conducted the experiments using slag and carbon-saturated hot metal in graphite crucibles, which would lead to the partial reduction of TiO_2. In most slag-gas equilibrium experiments, sub-oxides (Ti_2O_3) also exist due to the low oxygen potential.

A brief summary of models to calculate the sulfide capacity of slags is presented in Table 5. The optical basicity (Λ) based model was first proposed by Duffy et al. [113] to estimate the sulfide capacity of CaO-SiO_2-MgO-Al_2O_3 system and developed by other researchers [114-116] to apply in a wider range of composition and temperature, including TiO_2. Optical basicity indicates the degree of electron donation by the ligand in a coordinate bond, which can be measured experimentally from the frequency shifts in the ultra-violet (UV) spectra of

probe ions (i.e., Pb^{2+} and Tl^{+}) [117]. However, transition metal ions (i.e., Fe^{2+}, Fe^{3+}, Mn^{2+}, and Ti^{4+}) absorb intensely in the UV region, which means that the optical basicity of transition metal ions cannot be determined by UV spectra. In this case, Duffy [118] obtained their optical basicity values by using refractivity data: $\Lambda_{TiO_2} = 0.71 - 0.79$; $\Lambda_{FeO} = 0.86 - 1.08$; $\Lambda_{Fe_2O_3} = 0.73 - 0.81$; $and\ \Lambda_{MnO} = 0.94 - 1.03$. It should be noted that the optical basicity values of transition metal ions calculated from sulfide capacity data used in the models are different with each other, and a gap exits with the recommended value by Duffy [118] (see Table 5). Therefore, these models have limitations when applied to titania slags due to the lack of data. The quasi-chemical quadruplet approximation calculates the sulfide solubility via the thermodynamic activities of the component oxides and the Gibbs energies of the pure liquid components, which has been applied in the FactSage package [119]. A thermochemical model for sulfide capacity of slags has been developed by Moretti and Ottonello [120] based on the Toop-Samis polymeric approach combined with Flood-Grjotheim thermochemical cycle. This model claims a high heuristic capability without compositional limitations. Some models are not currently applicable to titania-containing slags, but there is a potential to extend it to titania-containing slags in future work, such as the KTH model [121], molecule coexistence theory model [122], and intelligent algorithms models [123-124]. The KTH model [121] predictions have shown a good agreement with the experimental results, but the calculation process needs lots of interaction parameters. Shi et al. [122] developed a model based on the ion and molecule coexistence theory for CaO-SiO_2-MgO-Al_2O_3 system without TiO_2. The rapid development of intelligent algorithms has attracted more and more researchers in the field of metallurgy. Ma et al. [123] and Xin et al. [124] established the sulfide capacity models based on artificial neural network and extreme learning machine for CaO-SiO_2-MgO-Al_2O_3 system, respectively. At the same time, the intelligent algorithms method based on big data has great limitations currently on titania slag with insufficient data.

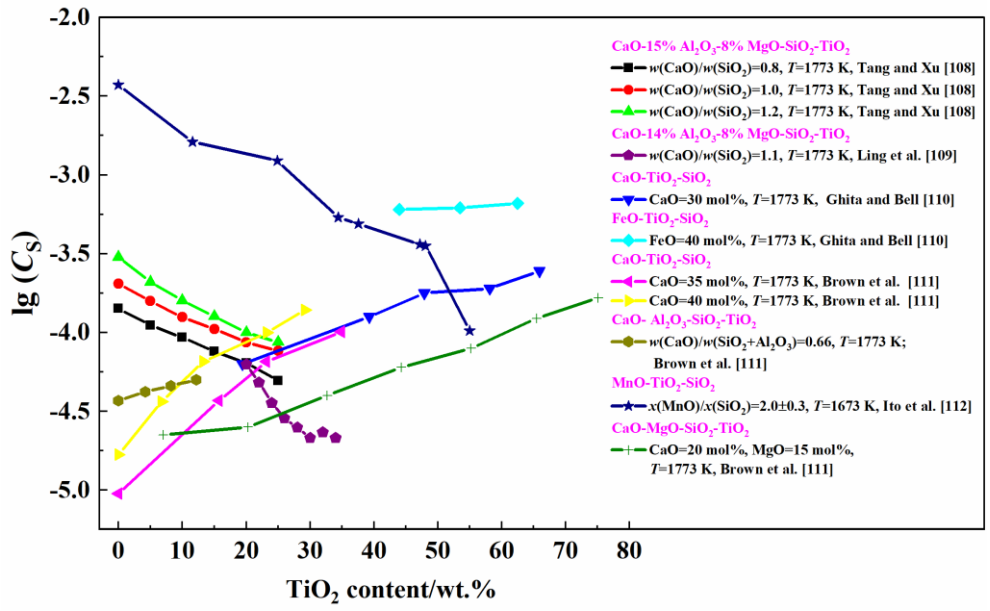

Fig. 10 Effect of TiO_2 on sulfide capacity of titania slags

Table 5 Summary of models to calculate sulfide capacity of titania-containing slags

Source	Description	Slag system
Sosinsky and Sommerville [114]	$\log C_S = (22{,}690 - 54{,}640\Lambda)/T + 43.6\Lambda - 25.2$ Recommended Λ value for transition metal oxides: $\Lambda_{TiO_2} = 0.61;\ \Lambda_{FeO} = 1.03;\ \Lambda_{Fe_2O_3} = 1.21;\ \Lambda_{MnO} = 0.90$	CaO-SiO_2-MgO-Al_2O_3-**TiO_2**-FeO-Fe_2O_3-MnO
Zhang et al. [115]	$\log C_S = -6.08 + 4.49/\Lambda + (15{,}893 - 15{,}864/\Lambda)\ /\ T$ Recommended Λ value for transition metal oxides: $\Lambda_{TiO_2} = 0.61;\ \Lambda_{FeO} = 1.24;\ \Lambda_{MnO} = 1.43;\ \Lambda_{CaF_2} = 0.88$	CaO-SiO_2-MgO-Al_2O_3-**TiO_2**-FeO-MnO-CaF_2
Young et al. [116]	$\log C_S = -13.913 + 42.84\Lambda - 23.82\Lambda^2 - \frac{11{,}710}{T} - 0.02223x_{SiO_2} - 0.02275x_{Al_2O_3};\ \Lambda < 0.8$ $C_S = -0.6261 + 0.4808\Lambda + 0.7917\Lambda^2 + \frac{1697}{T} - 2587\Lambda/T + 0.0005144x_{FeO};\ \Lambda \geq 0.8$ Recommended Λ value for transition metal oxides: $\Lambda_{TiO_2} = 0.65;\ \Lambda_{FeO} = 0.99;\ \Lambda_{Fe_2O_3} = 1.05;\ \Lambda_{MnO} = 1.05$	CaO-SiO_2-MgO-Al_2O_3-**TiO_2**-FeO-Fe_2O_3-MnO
Kang and Pelton [119]	Thermodynamic model in the framework of the modified quasi-chemical model, which has been successfully used in FactSage software	CaO-SiO_2-MgO-Al_2O_3-**TiO_2-Ti_2O_3**-FeO-Fe_2O_3-MnO
Moretti and Ottonello [120]	Thermochemical model in the framework of Toop-Samis polymeric model and Flood-Grjotheim thermochemical cycle	CaO-SiO_2-MgO-Al_2O_3-**TiO_2**-FeO-Fe_2O_3-MnO-P_2O_5-Cr_2O_3-Na_2O-K_2O

3. Structure of titania-containing metallurgical slags

The structure of silicate glasses and melts has been comprehensively reviewed by Mysen and Richet [125]. Although Mysen's work focuses on the geological sciences, it can also be extended to the metallurgical slags. Mills et al. [126], Sohn and Min [127], and Sajid et al. [128] reviewed the structure and properties relationship for silicate-based slags that are more

relevant to ironmaking and steelmaking processes. In this section, we have focused on the role of TiO_2 in the structure of titania-bearing slags.

The well-known 'ionic' and 'molecular' structure theories were developed to explain the properties of silicate-based slags, which cannot be satisfactorily applied to establish the structure of TiO_2-FeO slag systems. Handfield and Charette [37] compared the electrical conductivity of high titania slags with those of their corresponding solids and reported that their structure should be similar. As mentioned in Sect. 2.2, the principal constituents of solid high-titania slags are anosovite group minerals with M_3O_5 type structure (orthorhombic), tagirovite group minerals with M_2O_3 type structure (rhombohedral), and a small amount of glassy material. The variable valence of Ti in M_3O_5 or M_2O_3 types of structure results in the semiconducting properties. Reznichenko [70] suggested that the $[TiO_6^{8-}]$ anions are the main structural units of liquid high-titania slags in the view of that the TiO_6 octahedron is the basic structural unit of solid anosovite. Recently, from the molecular dynamics simulation results of liquid TiO_2 and TiO_2-FeO based slags [11, 56, 58, 129], the mean oxygen coordination number of Ti ($CN_{Ti\text{-}O}$) is near six ($^{[VI]}Ti$), which means that the primary structural unit is TiO_6 octahedron; the edge-sharing Ti-Ti has a stronger combining capacity than the corner-sharing Ti-Ti. However, the TiO_6 octahedron structure with $[TiO_6^{8-}]$ anions are not appropriate with the high electrical conductivity of these slags. Whether the structure of high titania slags is similar to their solids or most in the TiO_6 octahedron structure is not clear so far.

For the titania-silicate based glasses and melts, Ti^{4+} has the same valence as Si^{4+} in an oxidizing atmosphere. Since the ionic radius of Ti^{4+} (0.061 nm) is about twice that of Si^{4+} (0.026 nm), the Ti^{4+} might be unfit to replace the Si^{4+} in the network structure but prefer 6-fold coordinated titanium ($^{[VI]}Ti$) as a network modifier. However, the reality is not so simple. Henderson and Fleet [130] concluded that the spectra do not indicate the presence of $^{[VI]}Ti$, and found that the Ti^{4+} is 4-fold coordinated titanium ($^{[IV]}Ti$) via substitution of Si^{4+} in TiO_2-SiO_2 and TiO_2-$CaSiO_3$ glass systems at low TiO_2 content and have 5-fold coordinated titanium ($^{[V]}Ti$) at high TiO_2 content. However, the K-edge data from Li et al. [131] look difficult to reconcile with the $Ti^{4+} \leftrightarrow Si^{4+}$ substitution model but form separate clusters of TiO_4 tetrahedra. From an X-ray absorption near edge structure (XANES) study, Henderson et al. [132] reported that the $CN_{Ti\text{-}O}$ in Ca-titanosilicate glass is lower than that in K- and Na-systems, and the $CN_{Ti\text{-}O}$ depends on the TiO_2 content in these systems. The proportion of Ti^{4+} in high coordination increases with increasing TiO_2 content according to the Raman spectroscopy [133], neutron diffraction [134], and nuclear magnetic resonance (NMR)

examination data [135]. In X-ray absorption fine structure (XAFS) spectroscopy study by Farges et al. [136], $^{[V]}$Ti is the dominant species located in the distorted square pyramids in their studied glasses when TiO_2 is more than 16 wt.%. Raman spectroscopy is a useful tool to address the structure of glasses and melts. Many researchers have discussed the assignment of the bands related to Ti^{4+}, but still controversial. Mysen et al. [137] provided the recommended assignments of Ti-related Raman bands (see Table 6 as a brief summary), and reported that Ti^{4+} is 4-fold coordination in all the melts they studied. Based on the assignments of Ti-related Raman bands, Zheng et al. [138] and Pang et al. [30] investigated the structure of CaO-SiO_2-MgO(-Al_2O_3)-TiO_2 slags via Raman spectroscopy. Their results indicate that a considerable proportion of Ti^{4+} enters into the tetrahedron units as network formers, and $^{[V]}$Ti and $^{[VI]}$Ti also appear in their studied systems to act as network modifiers. However, the molecular dynamics simulation results of CaO-SiO_2-TiO_2(-MgO-Al_2O_3) slag conducted by Zhang et al. [139, 140] showed that the majority of titanium in $^{[VI]}$Ti is inconsistent with the Raman results. In the light of the above, Ti competes successfully with Si on oxygen bonding in titania-silicate based glasses and slags, resulting in the diversity of Ti-O polyhedral. Ti^{4+} can site in $^{[IV]}$Ti either as isolated clusters or in place of Si^{4+} in $^{[IV]}$Si, and it can also exist in higher coordination numbers. The relative abundance of the Ti-O polyhedral relates to TiO_2 content and the nature of metal cations.

Table 6 Recommended assignments of Ti-related Raman bands [136]

Frequencies of Raman bands/cm^{-1}	Recommended assignments
950−980	(Si,Ti)-coupled stretch band in a chain unit
~890	$^{-}$O-Ti-O^0 stretching vibrations
850−870	Stretching vibrations of titanyl bond in 5-coordinated Ti^{4+} or Ti-O bond $Ti_2O_6^{4-}$ chain units, or both
~810	Ti-O^{2-} stretching vibrations in TiO_4^{4-} monomers
~770	Ti-O stretching vibrations from depolymerized unit
~720	Deformation of O-Ti-O or O-(Si,Ti)-O in chain or sheet units or both
<700	Ti-O stretching vibrations of Ti in 6-fold coordination

4. Conclusion remarks and future work

There are mainly two types of metallurgical slag in the titanium resource utilization processes: the TiO_2-FeO based slags in EAF process and TiO_2-SiO_2 based slags in BF process. The TiO_2 has a significant effect on the slag physicochemical properties and structure:

1) Redox equilibrium of titanium results show a linear function between -log(Ti^{3+}/Ti^{4+}) and -

log(P_{O_2}) with a slope of about -4;

2) High titania slags have high liquidus temperature, which decreases with increasing FeO content. The liquidus temperature of titania-containing BF slag (TiO_2 >20 wt.%) is higher than that of ordinary BF slags due to the precipitation temperature of perovskite increases with increasing TiO_2 content and basicity. MgO and Al_2O_3 will increase the precipitation temperature of spinel that affects the liquidus temperature of slags.
3) The high titania slags have very low viscosities and are not sensitive to composition, but the viscosities increase sharply when solid phase is present. For TiO_2-SiO_2 based slags, the addition of TiO_2 typically decreases the viscosity under an inert/neutral atmosphere. The production of sub-oxides (Ti_2O_3 and TiO) causes a decrease in viscosity, but the formation of TiC increases the viscosity sharply, resulting in a more complicated viscosity of the titania slag under the reduction conditions.
4) The electrical conductivities of high titania slags are higher than those of silicate slags, indicating the semiconducting feature. The increase in TiO_2 increases the electrical conductivity of slags predominating the ionic conduction.
5) The typical high titania slags have a density range of 3.5 to 3.7 g/cm^3, and the density of titania-containing BF slags is in the range of 2.60 to 2.90 g/cm^3.
6) The TiO_2 acts as a surfactant to reduce the surface tension of slags, which is beneficial to slag foaming.
7) The thermal conductivity of the titania slags covers a range from 1.0 to 3.0 W m^{-1} °C^{-1}, and the heat capacity is between 700 to 1100 J kg^{-1} °C^{-1}.
8) The desulfurization capability of TiO_2 is weaker than those of MnO, CaO, MgO, and FeO, but stronger than those of Al_2O_3 and SiO_2. The optical basicity value of TiO_2 from refractivity data is inconsistent with the values from sulfide capacity data calculation.
9) The structure of high titania slags is not well understood yet. In titanosilicate based glasses and slags, Ti^{4+} can site in TiO_4 tetrahedra either as isolated clusters or in place of Si^{4+} in SiO_4 tetrahedra, and it can also exist in higher coordination numbers.

Due to the consumption of high-quality titanium resources, titania slag composition may be more complex and changeable. Research regarding titania-containing slag physicochemical properties will continue to be an important topic in the utilization of titanium resources processes. The slag with low TiO_2 grade (i.e., BF slag) has not been fully utilized, which not only results in environmental pollution, but also causes the waste of titanium resource. The recycling process and environmental concerns of this kind of slags will be more attractive in the future. To reduce the carbon footprint, hydrogen or natural gas

will be introduced into the reduction process to control CO_2 emissions. As the participation of hydrogen becomes critical, the slags may form hydroxyl which affects their physicochemical properties and structure. Physicochemical properties prediction models will continue to evolve and provide useful information to slag designer. In addition, model optimization requires accurate experimental data; thus, the model developer and experimentalist need to cooperate with each other to provide the latest evaluation of the slag systems. The current structure theories cannot explain the structure of high titanium slag satisfactorily; thus, a new structure theory is required for considering the ionic, polymeric and semiconducting features of the high titania slag to reconcile its properties. The current spectroscopic technologies have not yet fully clarified the role of TiO_2 in the structure of titanosilicate slags and glasses, and the computer simulation of titania slags structure is not mature.

Acknowledgements

The authors are pleased to acknowledge the support from the National Key R&D Program of China (No. 2018YFC1900500) and EPSRC (UK) under the grant number EP/N011368/1 (EPSRC Fellowship).

References

[1] D. Knittel, B.C. James, *Kirk-Othmer Encyclopedia of Chemical Technology.* 23 (1983) 98-130.
[2] R.L. Rudnick, S. Gao, *Treatise Geochem.* 3 (2003) 659.
[3] W. Zhang, Z. Zhu, C.Y. Cheng, *Hydrometallurgy* 108 (2011) 177-188.
[4] US Geological Survey, Mineral Commodity Summaries 2021, *https://pubs.er.usgs.gov/publication/mcs2021.*
[5] H. Sun, J. Wang, X. Dong, Q. Xue, *Metal. Int.* 17 (2012) 49-56.
[6] G. Buxbaum, Industrial inorganic pigments, John Wiley & Sons, USA, 2008.
[7] T. Ikeshima, *Titanium Science and Technology* 1 (1984) 3-14.
[8] M. Pourabdoli, S. Raygan, H. Abdizadeh, K. Hanaei, *Int. J. Miner. Process.* 78 (2006) 175-181.
[9] Z.F. Yuan, X. Yang, Z.X. Lu, J.N. Huang, Y.F. Pan, E.X. Ma, *J. Iron Steel Res. Int.* 14 (2007) No. 3, 1-6.
[10] K. Meijer, C. Zeilstra, C. Teerhuis, M. Ouwehand, J. van der Stel, *Trans. Indian Inst. Met*. 66 (2013) 475-481.
[11] K. Hu, X. Lv, S. Li, W. Lv, B. Song, K. Han, *Metall. Mater. Trans. B* 49 (2018) 1963-1973.
[12] C.G. Bai, *Study on some physical chemistry problems of blast furnace slag-bearing titania*, College of Materials Science and Engineering, Chongqing University, Chongqing, China, 2003.
[13] G. Tranell, O. Ostrovski, S. Jahanshahi, *in: Proc. 5th Intern. Conf. "Molten slags, fluxes and salts'*, Iron and Steel Society, Sydney, Australia, 1997, pp. 501-506.
[14] G. Tranell, O. Ostrovski, S. Jahanshahi, *Metall. Mater. Trans. B* 33 (2002) 61-67.
[15] W.D. Johnston, *J. Am. Ceram. Soc.* 48 (1965) 184-190.
[16] H.D. Schreiber, T. Thanyasiri, J.J. Lach, R.A. Legere, *Phys. Chem. Glasses* 19 (1978) 126–139.
[17] J. Tanabe, H. Suito, *Steel Res.* 63 (1992) 515-520.
[18] C. Ariyo, P. Gonzalez, L. Holappa, *Steel Res. Int.* 76 (2005) 284-287.
[19] K. Hu, X. Lv, Z. Yan, W. Lv, R. Zhang, J. Dang, Z. You, *Metall. Mater. Trans. B 50* (2019) 1841-1851.
[20] J. Pesl, R.H. Eriç, *Metall. Mater. Trans. B* 30 (1999) 695-705.
[21] J.M.A. Geldenhuis, P.C. Pistorius, J.S. Afr. Inst. Min. Metall. 99 (1999) 41-47.
[22] K. Ito, N. Sano, *Tetsu-to-Hagané* 67 (1981) 2131-2137.
[23] Y. Morizane, B. Ozturk, R.J. Fruehan, *Metall. Mater. Trans. B* 30 (1999) 29-43.
[24] P.C. Pistorius, J.S. Afr. Inst. Min. Metall. 108 (2008) 35-43.

[25] H. Kotzé, J.S. Afr. Inst. Min. Metall. 120 (2020) 121-130.
[26] P.C. Pistorius, C. Coetzee, *Metall. Mater. Trans. B* 34 (2003) 581-588.
[27] S. Seim, *Experimental investigations and phase relations in the liquid $FeTiO_3$-Ti_2O_3-TiO_2 slag system*, Department of Materials Technology, NTNU, 2011.
[28] Z. Yan, X. Lv, W. He, J. Xu, *ISIJ Int.* 57 (2017) 31-36.
[29] W.Z. Wang, K. Yu, *J. Northeast. Univ. (Nat. Sci.)* (1984) No. 4, 41-48.
[30] Z. Pang, X. Lv, J. Ling, Y. Jiang, Z. Yan, J. Dang, *Metall. Mater. Trans. B 51* (2020) 2348-2357.
[31] Z. Pang, X. Lv, Y. Jiang, J. Ling, Z. Yan, *Metall. Mater. Trans. B 51* (2020) 722-731.
[32] M.G. Frohberg, R. Weber, *Steel Res. Int.* 36 (1965) 477-480.
[33] A. Ohno, H.U. Ross, *Can. Metall. Quart.* 2 (1963) 259-279.
[34] H. Park, J.Y. Park, G.H. Kim, I. Sohn, *Steel Res. Int.* 83 (2012) 150-156.
[35] J.L. Liao, J. Li, X.D. Wang, Z.T. Zhang, *Ironmak. Steelmak.* 39 (2012) 133-139.
[36] I. Sohn, W. Wang, H. Matsuura, F. Tsukihashi, D.J. Min, *ISIJ Int.* 52 (2012) 158-160.
[37] G. Handfield, G.G. Charette, *Can. Metall. Quart.* 10 (1971) 235-243.
[38] M. Kato, S. Minowa, *Trans. Iron Steel Inst Jpn.* 9 (1969) 31-38.
[39] Y.U.P. Nikitin, V.M. Lopatin, L.N. Barmin, *Steel USSR* 3 (1973) No. 2, 122.
[40] G. Handfield, G.G. Charette, H.Y. Lee, *JOM* 24 (1972) 37-40.
[41] D. Xie, Y. Mao, Y. Zhu, in: VII International Conference on Molten Slags Fluxes and Salts, The South African Institute of Mining and Metallurgy, 2004, pp. 43-50.
[42] J. Van der Colf, D.D. Howat, J.S. Afr. Inst. Min. Metall. 79 (1979) 255-263.
[43] K. Mills, The estimation of slag properties, Department of Materials, Imperial College, London, UK, 2011.
[44] C. Han, M. Chen, W. Zhang, Z. Zhao, T. Evans, B. Zhao, *Metall. Mater. Trans. B* 47 (2016) 2861-2874.
[45] R. Khanna, V. Sahajwalla, *Treatise on process metallurgy, Volume 1: process fundamentals*, Elsevier Cambridge, 2013.
[46] G. Wu, *Modelling and experimental validation of the viscosity of liquid phases in oxide systems relevant to fuel slags*, Forschungszentrum Jülich GmbH, Zentralbibliothek, Germany, 2015.
[47] L. Gan, J. Xin, Y. Zhou, *ISIJ Int.* 57 (2017) 1303-1312.
[48] P.V. Riboud, Y. Roux, L.D. Lucas, H. Gaye, *Fachber. Huttenprax. Metallweiterverarbei.* 19 (1981) 859-869.
[49] T. Iida, H. Sakai, Y. Kita, K. Shigeno, *ISIJ Int.* 40 (2000) S110-S114.
[50] G. Urbain, *Steel Res.* 58 (1987) 111-116.
[51] G. Urbain, F. Cambier, M. Deletter, M.R. Anseau, *Trans. J. Br. Ceram. Soc.* 80 (1981) 139-141.
[52] K.C. Mills, S. Sridhar, *Ironmak. Steelmak.* 26 (1999) 262-268.
[53] G.H. Zhang, K.C. Chou, J.L. Zhang, *Ironmak. Steelmak.* 41 (2014) 47-50.
[54] Q.F. Shu, X. Zhang, K.C. Chou, *Ironmak. Steelmak.* 42 (2015) 641-647.
[55] Z. Yan, R.G. Reddy, X. Lv, Z. Pang, W. He, *Ironmak. Steelmak. 47* (2020) 203-209.
[56] H. Fan, D. Chen, P. Liu, H. Duan, Y. Huang, M. Long, T. Liu, *J. Non-Cryst. Solids* 493 (2018) 57-64.
[57] T. Wu, S. He, Y. Liang, Q. Wang, *J. Non-Cryst. Solids* 411 (2015) 145-151.
[58] Y. Kim, C. Nam, S. Kim, H. Jeon, *J. Non-Cryst. Solids* 552 (2021) 120308.
[59] K. Hu, K. Tang, X. Lv, J. Safarian, Z. Yan, B. Song, *Metall. Mater. Trans. B 52* (2021) 245-254.
[60] A. Einstein, *Ann. Phys.* 19 (1906) 289-306.
[61] R. Roscoe, *Br. J. Appl. Phys.* 3 (1952) 267.
[62] Y.L. Zhen, G.H. Zhang, K.C. Chou, *Metall. Mater. Trans. B* 46 (2015) 155-161.
[63] G.H. Zhang, Y.L. Zhen, K.C. Chou, *ISIJ Int.* 55 (2015) 922-927.
[64] A. Grau, D. Poggi, *Canadian Institute of Mining and Metallurgy, Metallurgical Society of CIM Annual Volume Featuring "Hydrogen in Metals" and "Titanium"* 17 (1978) 97-102.
[65] R. Desrosiers, F. Ajersch, A. Grau, Electrical conductivity of industrial slags of high titania content, *in: Proceedings of International Symposium on Metallurgical Slags, Part of the 19th Annual Conference of Metallurgists*, Canadian Institute of Mining and Metallugy, Nova Scotia, Canada, 1980.
[66] K. Hu, X. Lv, W. Yu, Z. Yan, W. Lv, S. Li, *Metall. Mater. Trans. B 50* (2019) 2982-2992.
[67] K. Mori, *Tetsu-to-Hagané* 42 (1956) 1024-1029.
[68] S.I. Denisov, V.S. Degtyarev, V.A. Reznichenko, *Izvest. Akad. Nauk SSSR, Metally 1* (1970) 80-82.
[69] H. Inouye, J.W. Tomlinson, J. Chipman, *Trans. Faraday Soc.* 49 (1953) 796-801.
[70] V.A. Reznichenko, *Izvest. Akad. Nauk SSSR, Metally* 5 (1967) 43-57.
[71] K. Narita, T. Onoye, T. Ishii, K.I. Uemura, *Tetsu-to-Hagané* 61 (1975) 2943-2951.
[72] N. Shinozaki, K. Mizoguchi, Y. Suginohara, *J. Jpn. Inst. Met.* 42 (1978) 162-168.
[73] Y.H. Shi, J.C. Wang, *Iron Steel Vanadium Titanium* (1987) No. 1, 56-60.
[74] N.F. Mott, *J. Non-Cryst. Solids* 1 (1968) 1-17.
[75] P.P. Evseev, A.F. Filippov, *Izv. Vyssh. Uchebn. Zaved., Chern. Met.* (1967) No. 3, 55-59.
[76] K. Mori, *Tetsu-to-Hagané* 46 (1960) 134-140.

[77] A.S. Churkin, Y.M. Tsikarev, G.A. Toporishchev, V.I. Lazarev, G.A. Khasin, *Protsessov (Sverdlovsk)* 7 (1979) 40–47.
[78] B.M. Lepinskikh, V.I. Musikhin, I.L. Korkiya, *Trudy. Inst. Met. Sverdlovsk* 18 (1969) 247-259.
[79] I.D. Sommerville, H.B. Bell, *Can. Metall. Quart.* 21 (1982) 145-155.
[80] Q. Jiao, N.J. Themelis, *Metall. Trans. B* 19 (1988) 133-140.
[81] G.H. Zhang, B.J. Yan, K.C. Chou, F.S. Li, *Metall. Mater. Trans. B* 42 (2011) 261-264.
[82] G.H. Zhang, K.C. Chou, *Metall. Mater. Trans. B* 41 (2010) 131-136.
[83] D.R. Gaskell, D.E. Laughlin, *Introduction to the thermodynamics of materials*, 6th ed., CRC Press, Boca Raton, USA, 2017.
[84] D.B. Dingwell, *J. Am. Ceram. Soc.* 74 (1991) 2718-2719.
[85] N. Ikemiya, J. Umemoto, S. Hara, K. Ogino, *ISIJ Int.* 33 (1993) 156-165.
[86] J. Xin, L. Gan, N. Wang, M. Chen, *Metall. Mater. Trans. B* 50 (2019) 2828-2842.
[87] Y. Liu, X. Lv, C. Bai, X. Zhang, *ISIJ Int.* 54 (2014) 2017-2024.
[88] Z.D. Pang, Y.Y. Jiang, J.W. Ling, X.W. Lv, Z.M. Yan. Int. J. Miner. Metall. Mater. (2021) https://doi.org/10.1007/s12613-021-2262-x.
[89] S.A. Nelson, I.S.E. Carmichael, *Contrib. Mineral Petrol.* 71 (1979) 117-124.
[90] R.A. Lange, I.S.E. Carmichael, *Geochim. Cosmochim. Acta* 51 (1987) 2931-2946.
[91] K.C. Mills, B.J. Keene, *Int. Mater. Rev.* 32 (1987) 1-120.
[92] Y. Linard, H. Nonnet, T. Advocat, *J. Non-Cryst. Solids* 354 (2008) 4917-4926.
[93] P. Kozakevitch, *Mem. Sci. Rev. Metall. XLVI-8* (1949) 505-516.
[94] A.I. Bochorishvili, S.B. Yakobashvili, *Svarochnoe Proizvodstvo* 1 (1968) 13-15.
[95] S.I. Popel, A.A. Deryabin, L.N. Saburov, M.V. Tarkhanov, *Tr. Uralsk. Nauchno-Issled. Inst. Chern. Metal* 12 (1971) 92.
[96] Y. Liu, X. Lv, C. Bai, B. Yu, *ISIJ Int.* 54 (2014) 2154-2161.
[97] Y.K. Zhu, Y.W. Mao, Z.X. Guo, G.H. Wang, Y.L. Dong, *Iron Steel Vanadium Titanium* (1983) No. 1, 14-18.
[98] R.E. Boni, G. Derge, *JOM* 8 (1956) 53-59.
[99] K.C. Mills, *in:* American Chemical Society Symposium Series Vol. 301, ACS, Washington DC, USA, 1986, pp. 195-214.
[100] M. Nakamoto, M. Hanao, T. Tanaka, M. Kawamoto, L. Holappa, M. Hamalainen, *ISIJ Int.* 47 (2007) 1075-1081.
[101] M. Nakamoto, A. Kiyose, T. Tanaka, L. Holappa, M. Hamalainen, *ISIJ Int.* 47 (2007) 38-43.
[102] M. Nakamoto, T. Tanaka, L. Holappa, M. Hamalainen, *ISIJ Int.* 47 (2007) 211-216.
[103] T. Tanaka, Thermodynamics of surface: relationship between surface properties and thermodynamic properties in bulk, *Bulletin of Iron & Steel Institute of Japan*, 2003.
[104] Y. Liu, X. Lv, C. Bai, *in: J.S. Carpenter (Eds.), Characterization of Minerals, Metals, and Materials,Springer, 201*5, pp. 217-224.
[105] H. Kotzé, P.C. Pistorius, J.S. Afr. Inst. Min. Metall. 110 (2010) 57-66.
[106] J. Heimo, A. Jokilaakso, M. Kekkonen, M. Tangstad, A. Støre, *Metall. Res. Technol.* 116 (2019) 635.
[107] C.J.B. Fincham, F.D. Richardson, *Proc. R. Soc. Lond. A* 223 (1954) 40-62.
[108] X. Tang, C. Xu, *ISIJ Int.* 35 (1995) 367-371.
[109] J. Ling, Z. Pang, Y. Jiang, Z. Yan, X. Lv, *Metall. Mater. Trans. B 52* (2021) 2786-2795.
[110] I. Ghita, H.B. Bell, *Ironmak. Steelmak.* 9 (1982) 239-243.
[111] S.D. Brown, R.J. Roxburgh, I. Ghita, H.B. Bell, *Ironmak. Steelmak.* 9 (1982) 163-167.
[112] M. Ito, K. Morita, N. Sano, *ISIJ Int.* 37 (1997) 839-843.
[113] J.A. Duffy, M.D. Ingram, I.D. Sommerville, *J. Chem. Soc., Faraday Trans.* 74 (1978) 1410-1419.
[114] D.J. Sosinsky, I.D. Sommerville, *Metall. Trans. B* 17 (1986) 331-337.
[115] G.H. Zhang, K.C. Chou, U. Pal, *ISIJ Int.* 53 (2013) 761-767.
[116] R.W. Young, Use of optical basicity concept for determining phosphorus and sulfur slag metal partitions, Technical Steel Research, Commission of European Communities, London, UK, 1991.
[117] J.A. Duffy, M.D. Ingram, *J. Am. Chem. Soc.* 93 (1971) 6448-6454.
[118] J. Duffy, *Ironmak. Steelmak.* 16 (1989) 426-428.
[119] Y.B. Kang, A.D. Pelton, *Metall. Mater. Trans. B* 40 (2009) 979-994.
[120] R. Moretti, G. Ottonello, *Metall. Mater. Trans. B* 34 (2003) 399-410.
[121] M.M. Nzotta, D. Sichen, S. Seetharaman, *ISIJ Int.* 38 (1998) 1170-1179.
[122] C.B. Shi, X.M. Yang, J.S. Jiao, C. Li, H.J. Guo, *ISIJ Int.* 50 (2010) 1362-1372.
[123] A. Ma, S. Mostaghel, K. Chattopadhyay, *ISIJ Int.* 57 (2017) 114-122.
[124] Z.C. Xin, J.S. Zhang, W.H. Lin, J.G. Zhang, Y. Jin, J. Zheng, J.F. Cui, Q. Liu, *Ironmak. Steelmak.* (2020) 275-283.
[125] B. Mysen, P. Richet, *Silicate glasses and melts: properties and structure*, Elsevier, 2005.

[126] K.C. Mills, M. Hayashi, L. Wang, T. Watanabe, in: S. Seetharaman (Eds.), *Treatise on Process Metallurgy, Vol. 1: Process Fundamentals*, Elsevier, 2014, pp. 149-286.
[127] I. Sohn, D.J. Min, *Steel Res. Int.* 83 (2012) 611-630.
[128] M. Sajid, C. Bai, M. Aamir, Z. You, Z. Yan, X. Lv, *ISIJ Int.* 59 (2019) 1153-1166.
[129] V.Van Hoang, *Phys. Status Solidi B* 244 (2007) 1280-1287.
[130] G.S. Henderson, M.E. Fleet, *The Canadian Mineralogist* 33 (1995) 399-408.
[131] D. Li, G.M. Bancroft, M.E. Fleet, X.H. Feng, *Phys. Chem. Miner.* 22 (1995) 115-122.
[132] G.S. Henderson, X. Liu, M.E. Fleet, *Phys. Chem. Miner.* 29 (2002) 32-42.
[133] B. Mysen, D. Neuville, *Geochim. Cosmochim. Acta* 59 (1995) 325-342.
[134] L. Cormier, G. Calas, D.R. Neuville, R. Bellissent, *J. Non-Cryst. Solids* 293-295 (2001) 510-516.
[135] S. Kroeker, D. Rice, J.F. Stebbins, *Am. Mineral.* 87 (2002) 572-579.
[136] F. Farges, G.E. Brown Jr., A. Navrotsky, H. Gan, J.J. Rehr, *Geochim. Cosmochim. Acta* 60 (1996) 3039-3053.
[137] B.O. Mysen, F.J. Ryerson, D. Virgo, *Am. Mineral.* 65 (1980) 1150-1165.
[138] K. Zheng, J. Liao, X. Wang, Z. Zhang, *J. Non-Cryst. Solids* 376 (2013) 209-215.
[139] S. Zhang, X. Zhang, C. Bai, L. Wen, X. Lv, *ISIJ Int.* 53 (2013) 1131-1137.
[140] S. Zhang, X. Zhang, W. Liu, X. Lv, C. Bai, L. Wang, *J. Non-Cryst. Solids* 402 (2014) 214-222.